Effects of light on molecular orientation of liquid crystals

1999 J. Phys.: Condens. Matter 11 R439

(http://iopscience.iop.org/0953-8984/11/41/201)

J. Phys.: Condens. Matter **11** (1999) R439–R487. Printed in the UK PII: S0953-8984(99)94069-9

REVIEW ARTICLE

Effects of light on molecular orientation of liquid crystals

F Simoni and O Francescangeli

Dipartimento di Scienze dei Materiali e della Terra and Istituto Nazionale per la Fisica della Materia, Università di Ancona, Via Brecce Bianche I-60131, Ancona, Italy

Received 5 July 1999

Abstract. A review of basic physical phenomena underlying the light-induced molecular reorientation in nematic liquid crystals is presented. A detailed description of the mechanisms of direct optical torque, photoisomerization and photorefractivity and of their effect on the macroscopic order of liquid crystals is reported. The first part of the article deals with the study of reorientation effects in transparent liquid crystalline materials. Here, the effects of photo-induced molecular reorientation are fully interpreted within the framework of classical electrodynamics and standard continuum theory of liquid crystals. We investigate the peculiar properties related to the macroscopic anisotropy and the collective behaviour of liquid crystals that result in extraordinarily large nonlinear optical response. Afterwards, the behaviour of liquid crystals in the presence of light absorption is considered and the related reorientation effects are discussed. We give a review of the wide phenomenology which is met in liquid crystals when doped with absorbing azo-dye molecules. The photoisomerization process that in this case drives the evolution of the dye–liquid crystal mixture consequent to the interaction with the light is discussed in detail. Finally, the relatively new field of photorefractivity in liquid crystals as a source of molecular reorientation is considered. We describe the different mechanisms contributing to the creation of a space-charge field such as conductivity anisotropy, dielectric anisotropy and photocharge production. A theoretical discussion of the fundamental mechanisms regulating the dc-field-assisted optically induced space-charge fields and the optical molecular reorientation in nematic liquid crystal films is also given.

1. Introduction

It is well known that molecular reorientation is an important mechanism to induce a nonlinear optical (NLO) response in fluids. Even if the medium is macroscopically isotropic, molecules are often anisotropic, therefore the optical field will align them because of the interaction with the permanent or induced dipoles of the molecules. As a consequence, a molecular redistribution also occurs due to the interaction among the induced dipoles. The reorientation and redistribution of molecules give rise to a change of the molecular polarizabilities that depends on the field strength and may lead to effects such as nonlinear scattering or nonlinear birefringence. In general this mechanism leads to a NLO polarization driven by a $\underline{\chi}^{(3)}$ tensor of the order of 10^{-14}–10^{-15} esu.

As already pointed out these effects are observed in materials which are isotropic but are constituted of anisotropic molecules. The peculiarity of liquid crystals (LCs) is that not only they are made of anisotropic molecules but also they keep this anisotropy on a macroscopic scale. Thus, even if the above cited phenomenon of molecular reorientation may occur, much stronger effects can take place which are related to the macroscopic anisotropy and the collective behaviour of these materials. In this paper we will be concerned with these effects, which are peculiar to LCs and lead to extraordinarily large NLO response. We will review the main

0953-8984/99/410439+49$30.00

properties of the light-induced phenomena which strongly affect the macroscopic order of LCs. To this end we will not follow the microscopic point of view that deals with the single molecule and its reorientation but rather we will undertake a macroscopic approach making use of the concept of molecular director $\boldsymbol{n}$. In fact, a liquid crystal (LC) being a fluid material characterized by long-range orientational order (nematic LC), it is possible to define a unit vector $\boldsymbol{n}$, called the molecular director, which represents the average direction of the molecular long axis. Then, the collective properties of the system can be studied within the frame of a continuum theory so that the macroscopic physical properties vary according to the local orientation of the director $\boldsymbol{n} = \boldsymbol{n}(\boldsymbol{r})$, $\boldsymbol{r}$ being the position vector. Of course, this model applies as long as the average of $\boldsymbol{n}$ over a large number of molecules is meaningful, i.e. as long as variations of $\boldsymbol{n}$ occur over distances much larger than the molecular scale. In this way the light-induced effects on the orientation of an LC are investigated as the effects on the average molecular direction, i.e. the way $\boldsymbol{n}(\boldsymbol{r})$ is modified by the interaction with light.

As a matter of fact light can interact in several ways with an LC, producing variations of the director orientation. However, in the following we will consider only those phenomena in which the optical field of the electromagnetic wave interacting with the medium plays a direct crucial role. In contrast, effects where reorientation is an indirect consequence of energy absorption, like thermal reorientation, will be disregarded. In particular the following mechanisms of reorientation will be reviewed:

(a) direct optical torque due to light field;
(b) photoisomerization;
(c) photorefractivity.

We believe that at the present state of knowledge these are the basic phenomena occurring in the interaction of light with LCs.

2. Optical torque

2.1. Experimental observations

In 1980 Zel'dovich and coworkers [1] announced the discovery of giant optical nonlinearities in nematic LCs. By detecting a self-focusing effect they measured a nonlinear dielectric permittivity nine orders of magnitude higher than it is in a strong nonlinear liquid like CS_2. Almost at the same time Khoo and Zhuang [2] and Zolot'ko *et al* [3] reported similar results in experiments dealing with the nonlinear optical response of nematics, and Shen and coworkers [4] reported the observation of the optical Fredericksz transition. From these observations it was soon clear that an optical field could act on the liquid crystal molecules in a way very similar to a low frequency electric or magnetic field, the observed nonlinear optical behaviour being just the effect of a change of refractive index consequent to a change of the director orientation. After the first demonstrations, many other experiments were performed [5–27] mainly with two different aims. The first one was the exploitation of the huge nonlinear response of LCs in order to study nonlinear optical effects, such as self-phase modulation and optical bistability, in simple geometries; the second one was the use of the nonlinear response to obtain additional information on the material parameters such as elastic constants, viscosities etc. It is not the aim of the present paper to review all the possible studies related to this optical reorientation process; rather, starting from the experimental evidence of this effect, we want to give a presentation of the method that can be used to treat the problem and to underline its main consequences.

The theoretical description given below is based on simple but important experimental observations. These experiments can be performed either by looking at self-induced effects,

thus measuring the optical nonlinear response on a single light beam, or by probing with a second beam the reorientation induced by the first one. The self-induced effect is well demonstrated in the self-focusing geometry: a lens is used to focus the light beam before the LC sample (figure 1) and the beam diameter is measured in the far field after crossing the sample. The change in the beam diameter of an incident Gaussian beam demonstrates that the refractive index n depends on the intensity I as $n(I) = n^0 + n_2 I$. In fact, when $n_2 I > 0$ the refractive index will be a maximum in the centre of the beam, decreasing to its minimum value n^0 at the edges. This means that the LC cell acts as a nonlinear positive lens whose intensity-dependent focal length f can be experimentally measured; in this way $f^{-1}(I)$ gives a direct measurement of n_2 (figure 2).

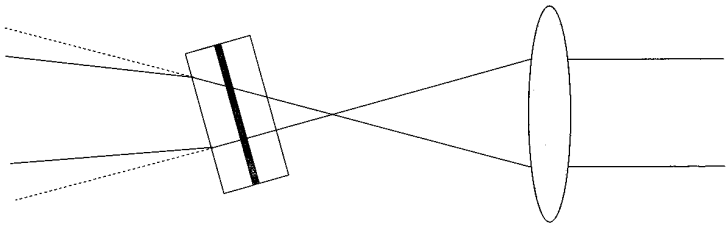

Figure 1. Geometry of the self-focusing effect in liquid crystals.

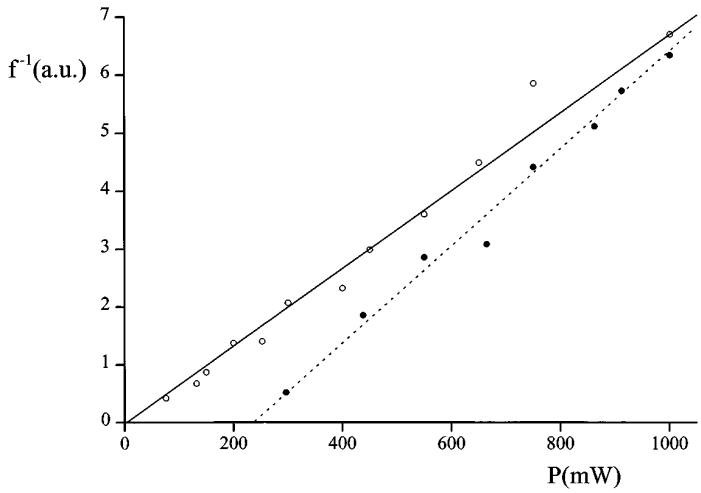

Figure 2. Inverse focal length of the liquid crystal as a function of the incident power. The circles correspond to a hybrid aligned (HAN) LC cell, the dots to a homeotropic (HOM) LC cell. The two sets of data were measured with the same material and cell thickness. After Simoni and Bartolino [17].

A key point of this experiment is the observation of the self-induced effect only in the extraordinary wave passing through the anisotropic liquid crystalline medium, whereas no change is detected in the ordinary wave whose refractive index is constant and equal to $n_\perp$.

For the extraordinary wave the refractive index is given by

$$n = \frac{n_\parallel n_\perp}{n_\parallel^2 \cos^2\theta + n_\perp^2 \sin^2\theta} \tag{1}$$

where θ is the angle between the light wavevector and the molecular director $\boldsymbol{n}$ and the symbols $\parallel$ and $\perp$ stand for parallel and perpendicular to $\boldsymbol{n}$, respectively. Therefore, the experimental results say that θ changes with the intensity.

As already mentioned, another way of showing the optical reorientation is to make use of a pump–probe technique, which is able to detect very small effects. In this case, one intense (pump) beam is used to induce the reorientation and a second weak (probe) beam to detect it (figure 3). The quantity measured is the intensity of the probe beam when the sample is placed between crossed polarizers: in this configuration any change of the director orientation changes the optical phase shift between the ordinary and extraordinary waves of the probe beam and gives rise to a signal transmitted by the analyser. Again, the detected phase shift ψ can be related to the change of refractive index due to a change of orientation, since it is

$$\psi = \frac{2\pi}{\lambda}\int_0^d n(z)\,\mathrm{d}z \tag{2}$$

with d being the thickness of the LC cell.

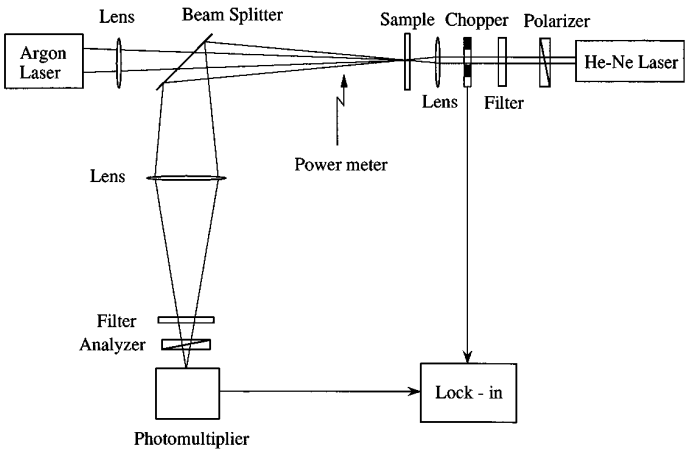

Figure 3. Schematic representation of a pump–probe experiment.

The conclusion of these observations is that light can exert an 'optical torque' on the LC molecules thus changing their orientation. Accordingly, we speak of 'optical torque' every time the electric field of an electromagnetic wave acts on the liquid crystal director and eventually reorients it. We are not talking here about conventional molecular reorientation which may occur in any fluid material due to the simple coupling between the molecule's dipole moment and the applied field, but we are considering only the peculiar feature of LCs, that is, the collective reorientation. Actually, the origin of the phenomenon is the same as in other fluids even though it seems difficult to work out how an optical field oscillating at frequencies between 10^{14} and 10^{15} Hertz is able to induce a collective reorientation with response time of the order of seconds. As a matter of fact, if one considers the dipole moment $\boldsymbol{p}$ induced by the oscillating field $\boldsymbol{E} = \boldsymbol{E}_0\,\mathrm{e}^{\mathrm{i}\omega t}$, it is possible to write it as $\boldsymbol{p} = \underline{\boldsymbol{\alpha}}\boldsymbol{E} = \boldsymbol{p}_0\,\mathrm{e}^{\mathrm{i}\omega t}$, where $\underline{\boldsymbol{\alpha}}$ is the molecular polarizability tensor. As a consequence the torque $\tau = \boldsymbol{p} \times \boldsymbol{E}$ acting on the molecule is given by $\tau(t) = (\boldsymbol{p}_0 \times \boldsymbol{E}_0)\cos^2\omega t$. Since the collective motion is very slow in comparison with the optical period, one has to consider the time average of $\boldsymbol{\tau}(t)$, i.e. $\langle\boldsymbol{\tau}(t)\rangle = (1/2)(\boldsymbol{p}_0 \times \boldsymbol{E}_0)$. Two important features then become apparent: (i) the high frequency optical field may induce a low frequency collective reorientation motion; (ii) far

from saturation, the optical torque is proportional to the square of the electric field (since p_0 is proportional to E_0). At first sight the only difference with respect to the effect induced by a static or low frequency electric field is the factor $1/2$ from the time average. Really, this simple consideration may be misleading since the interaction between light and LC molecules is a complex problem that involves the elasticity of the medium and the properties of wave propagation in an anisotropic inhomogeneous medium, giving rise to phenomena which have no counterpart in the low frequency case. The corresponding analytical problem has closed form solutions only under specific approximations as discussed in detail in the following section.

2.2. Theoretical approach

A rigorous description of the interaction between light and LC needs the formulation of the free energy density of the system followed by minimization through the Euler–Lagrange equations [28]. The elastic properties of the medium are described by the Frank elastic free energy density [29]:

$$F_K = \frac{K_1}{2}(\nabla \boldsymbol{n})^2 + \frac{K_2}{2}(\boldsymbol{n} \cdot \boldsymbol{\nabla} \times \boldsymbol{n})^2 + \frac{K_3}{2}(\boldsymbol{n} \times \boldsymbol{\nabla} \times \boldsymbol{n})^2 \tag{3}$$

where K_1, K_2, K_3 are the splay, twist and bend elastic constants.

Besides F_K we have to consider the contribution F_{OPT} from the interaction with the light field, and then proceed to minimization of the total free energy density

$$F = F_K + F_{OPT}. \tag{4}$$

Additionally, it is necessary to take into account proper boundary conditions and, in the case of finite anchoring energy, also the contribution to the free energy density coming from the interaction with the boundary surfaces. However, in many circumstances the *strong anchoring* approximation is fulfilled, which means that variations of the director orientation are negligible near the surfaces. In this case, the chosen geometry fixes the director orientation at the boundaries. We consider first this situation.

Before investigating in detail the form of F_{OPT} it is better to take a look at the Euler–Lagrange equations obtained by minimization of F with the constrain $\boldsymbol{n}(\boldsymbol{r}) \cdot \boldsymbol{n}(\boldsymbol{r}) = 1$. These are

$$\sum_\beta \frac{\partial}{\partial x_\beta} \frac{\partial F}{\partial(\partial n_\alpha / \partial x_\beta)} - \frac{\partial F}{\partial n_\alpha} = -\lambda(\boldsymbol{r}) n_\alpha \tag{5}$$

where $\alpha = x, y, z$ and $\lambda(\boldsymbol{r})$ is an arbitrary function of $\boldsymbol{r}$. In the absence of any electromagnetic wave the equilibrium configuration of $\boldsymbol{n}$ is obtained by placing $F = F_K$ in equation (4) and the boundary conditions will force $\boldsymbol{n}$ to have a specific orientation. In this way, as suggested by De Gennes [29], it is possible to define a molecular field vector $\boldsymbol{h}$ such that $\boldsymbol{n}$ is parallel to $\boldsymbol{h}$ when no field is applied

$$h_\alpha = \sum_\beta \frac{\partial}{\partial x_\beta} \frac{\partial F}{\partial(\partial n_\alpha / \partial x_\beta)} - \frac{\partial F}{\partial n_\alpha} = -\lambda(\boldsymbol{r}) n_\alpha. \tag{6}$$

Accordingly, the molecular field produces an effect similar to that produced by an electric or magnetic field acting on the director with a torque that is zero only when $\boldsymbol{n}$ is parallel to $\boldsymbol{h}$ so that at equilibrium it is $\boldsymbol{h} = -\lambda(\boldsymbol{r})\boldsymbol{n}$. With this definition, the equilibrium condition expressed by equation (5) can be written in the form

$$\boldsymbol{n} \times \boldsymbol{h} = 0. \tag{7}$$

Equation (7) allows us to define the *elastic torque* as

$$\boldsymbol{\Gamma}_K = \boldsymbol{n} \times \boldsymbol{h}. \tag{8}$$

Then, with no field applied the equilibrium is obtained when the elastic torque vanishes. In order to understand more deeply the meaning of this statement it is useful to consider the following important example. Under the one constant approximation ($K_1 = K_2 = K_3 = K$) equation (4) leads to:

$$\boldsymbol{h} = K\nabla^2\boldsymbol{n}. \tag{9}$$

In the case of planar distortion, $\boldsymbol{n}$ depends on a single parameter which can be chosen to be the tilt angle θ between the director and the axis normal to the boundary surfaces, z. Then we have

$$\begin{aligned} n_x &= \sin\theta(z) \\ n_z &= \cos\theta(z) \end{aligned} \tag{10}$$

and considering a uniform distortion in a transversal plane, i.e. $\partial/\partial x = \partial/\partial y = 0$, we obtain

$$\begin{aligned} h_x &= K\{-\sin\theta(z)[\mathrm{d}\theta/\mathrm{d}z]^2 + \cos\theta(z)[\mathrm{d}^2\theta/\mathrm{d}z^2]\} \\ h_z &= K\{-\cos\theta(z)[\mathrm{d}\theta/\mathrm{d}z]^2 - \sin\theta(z)[\mathrm{d}^2\theta/\mathrm{d}z^2]\} \end{aligned} \tag{11}$$

and the elastic torque becomes:

$$\boldsymbol{\Gamma}_K = \boldsymbol{n} \times \boldsymbol{h} = (h_x n_z - h_z n_x)\boldsymbol{j} = K[\mathrm{d}^2\theta/\mathrm{d}z^2]\boldsymbol{j}. \tag{12}$$

The equilibrium condition $\boldsymbol{\Gamma}_K = 0$ imposes $\mathrm{d}^2\theta/\mathrm{d}z^2 = 0$, i.e. $\mathrm{d}\theta/\mathrm{d}z =$ constant, which will be fixed by the boundary conditions. In case of equal orientation on both surfaces ($\boldsymbol{n}$ parallel to the boundaries, i.e. planar alignment, or $\boldsymbol{n}$ perpendicular to the boundaries, i.e. homeotropic alignment) this condition becomes $\mathrm{d}\theta/\mathrm{d}z = 0$ and a uniform planar or homeotropic orientation is obtained through the whole sample, thus realizing a single-crystal-like orientation over macroscopic distances.

Following this approach to describe the collective orientation of the liquid crystal molecules we want to write the effect of the electromagnetic field as an additional torque $\boldsymbol{\Gamma}_{OPT}$ acting on the director such as the new equilibrium condition is given by

$$\boldsymbol{\Gamma}_K + \boldsymbol{\Gamma}_{OPT} = 0. \tag{13}$$

This simple relationship allows us to work out the observed effects of optical reorientation in LCs from a macroscopic mechanical point of view. Under the action of an electromagnetic wave the director field takes a new equilibrium configuration; after the optical field is switched off (so that Γ_{OPT} becomes zero), the director field goes back to the initial orientation due to the elastic torque.

However, it is not easy to obtain an explicit expression for Γ_{OPT} since the problem has analytical solutions only in peculiar conditions. In order to explain the physics of these optical reorientation phenomena we will keep the approximation of *in plane* director reorientation which allows us to use only one Euler angle to define $\boldsymbol{n}$ locally. The wave nature of the exciting field represents another problem since it makes the optical field not uniform inside the medium. If the director distortion takes place over distances larger than the wavelength, as usually occurs, then it is possible to use the geometrical optics approximation (GOA) [30]. Under these assumptions we will work out the expression of F_{OPT} and will identify the *optical torque* as

$$\Gamma_{OPT} = \partial F_{OPT}/\partial\theta \tag{14}$$

from basic definitions of dynamical quantities.

In order to obtain F_{OPT} let us first recall the relationship between the electric induction and the electric field

$$\boldsymbol{D} = \varepsilon_\perp \boldsymbol{E} + \Delta\varepsilon(\boldsymbol{n}\cdot\boldsymbol{E})\boldsymbol{n} \tag{15}$$

with $\Delta\varepsilon = \varepsilon_\parallel - \varepsilon_\perp$, and the energy density of the interaction with the field

$$U_E = -\frac{1}{4\pi}\int \boldsymbol{D}\cdot \mathrm{d}\boldsymbol{E}. \tag{16}$$

Actually the electromagnetic wave carries also a magnetic field which interacts with the medium. However, even if the interaction energy is equal to the one due to the electric field, the orienting action is negligible and therefore its contribution can be disregarded.

Then, when considering the oscillating field $\boldsymbol{E} = \frac{1}{2}(\boldsymbol{E}_0\,\mathrm{e}^{\mathrm{i}\omega t} + \mathrm{CC})$ it is straightforward to obtain

$$F_E = -\frac{1}{16\pi}\varepsilon_{ik}E_iE_k^* = -\varepsilon_\perp\frac{|\boldsymbol{E}|^2}{16\pi} - \frac{\Delta\varepsilon}{16\pi}(\boldsymbol{n}\cdot\boldsymbol{E})(\boldsymbol{n}\cdot\boldsymbol{E}^*) \tag{17}$$

where minimization is carried out by considering E as a fixed parameter. It is convenient here to use the Euler–Lagrange equations in the following form:

$$\frac{\partial F}{\partial q^i} - \sum_\beta \frac{\partial}{\partial x_\beta}\frac{\partial F}{\partial(\partial q^i/\partial x_\beta)} = 0 \tag{18}$$

where q^i are the chosen thermodynamical coordinates which in our case correspond to the Euler angles of the director. Moreover, for planar reorientation they reduce to a single tilt angle θ. Finally, the total free energy density can be written as:

$$F = F_K + F_E = \frac{K_1}{2}\sin^2\theta\left(\frac{\mathrm{d}\theta}{\mathrm{d}z}\right)^2 + \frac{K_3}{2}\cos^2\theta\left(\frac{\mathrm{d}\theta}{\mathrm{d}z}\right)^2 - \varepsilon_\perp\frac{|\boldsymbol{E}|^2}{16\pi} - \frac{\Delta\varepsilon}{16\pi}(\boldsymbol{n}\cdot\boldsymbol{E})(\boldsymbol{n}\cdot\boldsymbol{E}^*) \tag{19}$$

where $\boldsymbol{E} = \{E_x\boldsymbol{u}_x + E_z\boldsymbol{u}_z\}\,\mathrm{e}^{\mathrm{i}\{[(\omega s/c)x + k_z z] - \omega t\}}$, with $\boldsymbol{k}_0 = k_x\boldsymbol{u}_x + k_z\boldsymbol{u}_z$ the vacuum wavevector and $k_x = \omega s/c$, with $s = \sin\beta_0$ and β_0 the external incidence angle. Minimization of F leads to:

$$(K_1\sin^2\theta + K_3\cos^2\theta)\left(\frac{\mathrm{d}^2\theta}{\mathrm{d}z^2}\right) - (K_3 - K_1)\sin\theta\cos\theta\left(\frac{\mathrm{d}\theta}{\mathrm{d}z}\right)^2 + \frac{\Delta\varepsilon}{16\pi}\{\sin 2\theta(|E_x|^2 - |E_z|^2) + \cos 2\theta|E_xE_z^* + E_x^*E_z|\} = 0. \tag{20}$$

From a qualitative point of view the difference with respect to the low frequency case is the requirement for the field to fulfil the wave equation. Under GOA the solution can be written as

$$(K_1\sin^2\theta + K_3\cos^2\theta)\left(\frac{\mathrm{d}^2\theta}{\mathrm{d}z^2}\right) - (K_3 - K_1)\sin\theta\cos\theta\left(\frac{\mathrm{d}\theta}{\mathrm{d}z}\right)^2 + \frac{\Delta\varepsilon}{16\pi}h(\theta) = 0 \tag{21}$$

where $h(\theta)$ is defined as:

$$h(\theta) = \left[\frac{g_0^2 g - s^2(\varepsilon_\perp\varepsilon_\parallel) - g\Delta\varepsilon^2\sin^2\theta\cos^2\theta - 2sg^{1/2}\Delta\varepsilon(\varepsilon_\perp\varepsilon_\parallel)^{1/2}\sin\theta\cos\theta}{g_0^2 g^{1/2}}\right]A^2\sin 2\theta - \left[\frac{s(\varepsilon_\perp\varepsilon_\parallel)^{1/2} + g^{1/2}\Delta\varepsilon\sin\theta\cos\theta}{g_0}\right]2A^2\cos 2\theta \tag{22}$$

with $g = \varepsilon_\perp + \Delta\varepsilon\cos^2\theta - s^2$, $g_0 = \varepsilon_\perp + \Delta\varepsilon\cos^2\theta = \varepsilon_\parallel - \Delta\varepsilon\sin^2\theta$ and A a constant parameter proportional to the light intensity and defined as

$$A^2 = (8\pi/c)(\varepsilon_\perp\varepsilon_\parallel)^{-1/2}I\cos\beta_0. \tag{23}$$

At normal incidence we can further simplify the problem and obtain

$$h(\theta) = \frac{2A^2 \sin\theta\cos\theta}{g_0^{3/2}}\varepsilon_\parallel\varepsilon_\perp. \tag{24}$$

Finally, using the elastic anisotropy $K_a = 1 - K_1/K_3$ we have:

$$(1 - K_a \sin^2\theta)\frac{\mathrm{d}^2\theta}{\mathrm{d}z^2} - K_a \sin\theta\cos\theta\left(\frac{\mathrm{d}\theta}{\mathrm{d}z}\right)^2 + I\frac{(\varepsilon_\parallel\varepsilon_\perp)^{1/2}\Delta\varepsilon\sin\theta\cos\theta}{cK_3(\varepsilon_\perp + \Delta\varepsilon\cos^2\theta)^{3/2}} = 0. \tag{25}$$

In this equation the first two terms represent the elastic torque, $\Gamma_K = \partial F_K/\partial\theta$, whereas the last one is the optical torque $\Gamma_{OPT} = \partial F_{OPT}/\partial\theta$. Accordingly, equation (25) is simply the mechanical equilibrium equation $\mathbf{\Gamma}_K + \mathbf{\Gamma}_{OPT} = 0$. Integration is easily performed to give

$$(1 - K_a \sin^2\theta)\left(\frac{\mathrm{d}\theta}{\mathrm{d}z}\right)^2 + f(\theta, I) = c^2 \tag{26}$$

where

$$f(\theta, I) = I\frac{2}{cK_3}\frac{(\varepsilon_\parallel\varepsilon_\perp)^{1/2}}{(\varepsilon_\perp + \Delta\varepsilon\cos^2\theta)^{1/2}} \tag{27}$$

and c^2 is an integration constant to be determined from the boundary conditions. θ_1 and θ_2 being the pretilt angles, integration of equation (26) gives

$$\int_{\theta_1}^{\theta_2}\left[\frac{1 - K_a\sin^2\theta}{c^2 - f(\theta, I)}\right]^{1/2}\mathrm{d}\theta = d \tag{28}$$

where d is the sample thickness. In the case of strong anchoring, θ_1 and θ_2 are fixed by the experimental geometry ($\theta_1 = \theta_2 = 0$ for the homeotropic cell, $\theta_1 = \theta_2 = \pi/2$ for the planar cell, and $\theta_1 = 0$ and $\theta_2 = \pi/2$ for the hybrid aligned cell).

After calculating c^2 from equation (28), the director distribution at a given light intensity $\theta(z, I)$ is worked out from the integral equation:

$$\int_{\theta_1}^{\theta(z)}\left[\frac{1 - K_a\sin^2\theta'}{c^2 - f(\theta', I)}\right]^{1/2}\mathrm{d}\theta' = z + d/2 \tag{29}$$

assuming the $z = 0$ plane at the centre of the cell.

Once we know the actual director orientation throughout the nematic cell at a given intensity, it is possible to investigate the different effects which arise as a consequence of the applied optical torque. As a matter of fact, upon changing the boundary conditions (pretilt angles and anchoring energy) and polarization state of the impinging light, many different situations occur, some of which have not been studied yet. For this reason, we will review only the most important effects which are somehow representative of the different categories which these phenomena may belong to.

As far as light propagation is concerned, the main effect of the collective reorientation is a huge change of the refractive index of the extraordinary wave travelling through the liquid crystal sample. Such a variation is so big as compared to conventional nonlinear materials that the related optical effects justify the denomination of giant optical nonlinearities. The nonlinear optical response can be easily worked out when the function $\theta(z, I)$ is known. The dielectric permittivity at optical frequencies of the extraordinary wave travelling in the liquid crystal can be written as

$$\varepsilon[\theta(z)] = \frac{\varepsilon^2 - (\Delta\varepsilon/2)^2}{\varepsilon + (\Delta\varepsilon/2)\cos 2\theta(z)} \tag{30}$$

where $\varepsilon = (\varepsilon_\parallel + \varepsilon_\perp)/2$. The nonlinear part of the dielectric permittivity is

$$\delta\varepsilon(z, I) = \varepsilon(z, I) - \varepsilon(z, 0) \tag{31}$$

that is:

$$\delta\varepsilon[\theta(z, I)] = \frac{\Delta\varepsilon}{2}\left[\varepsilon^2 - \left(\frac{\Delta\varepsilon}{2}\right)^2\right]\frac{\cos 2\theta(z, 0) - \cos 2\theta(z, I)}{[\varepsilon + (\Delta\varepsilon/2)\cos 2\theta(z, 0)][\varepsilon + (\Delta\varepsilon/2)\cos 2\theta(z, I)]} \tag{32}$$

where $\theta(z, 0)$ is the tilt angle distribution at zero intensity and $\theta(z, I)$ is the distribution under illumination of intensity I. Equation (32) gives a *local* value of the nonlinear part of the dielectric permittivity; the effect of all the sample is obtained by averaging $\delta\varepsilon$ over the cell thickness

$$\langle\delta\varepsilon\rangle = \frac{1}{d}\int_{-d/2}^{d/2}\delta\varepsilon(z, I)\,\mathrm{d}z. \tag{33}$$

As a consequence we obtain a nonlinear part in the refractive index given by

$$\delta n = \frac{\delta\varepsilon}{2n_{eff}^0} \tag{34}$$

where $n_{eff}^0 = n(z, 0)$ is the zero intensity refractive index of the extraordinary wave.

The dependence of $\delta\varepsilon$ and δn on the optical field can be made explicit by means of a series expansion of equations (33) and (34). In this case (small reorientation), a square dependence on the field (linear in the intensity) is obtained. However, the complete analytical expressions are necessary to describe the behaviour at higher intensity when saturation occurs. As an example figure 4 reports the quantity $\langle\delta\varepsilon\rangle$ calculated for a hybrid aligned cell ($\theta_1 = 0, \theta_2 = \pi/2$) under strong anchoring conditions, against the light intensity I, at normal incidence. As mentioned, a linear dependence on I (i.e. square dependence on the field) is apparent at low intensities whereas a saturation value is approached with increasing I. This behaviour is easily explained in terms of an almost complete alignment of the molecules along the field. The light power required to reach saturation is of the order of 10^4 W cm^{-2} and can be obtained by slightly focusing on the sample a low power c.w. laser beam.

2.3. Small reorientations

In order to work out the role played by the material parameters in the nonlinear response, it is useful to consider the small reorientation approximation and obtain an analytical expression for the nonlinear permittivity. As an example, let us consider the homeotropic nematic cell where initially the director is aligned along a direction perpendicular to the boundary surfaces ($\theta_1 = 0$,$\theta_2 = 0$). By linearization of equation (20), in the limit $\theta \ll 1$, we obtain

$$K_3\left(\frac{\mathrm{d}^2\theta}{\mathrm{d}z^2}\right) + \frac{\Delta\varepsilon}{16\pi}\{2\theta(|E_x|^2 - |E_z|^2) + |E_x E_z^* + E_x^* E_z|\} = 0. \tag{35}$$

Using the field calculated within the GOA, this latter reduces to

$$K_3\left(\frac{\mathrm{d}^2\theta}{\mathrm{d}z^2}\right) + H(\theta) = 0 \tag{36}$$

where

$$H(\theta) = A^2\frac{\Delta\varepsilon}{8\pi}\left\{\frac{\varepsilon_\perp(\varepsilon_\parallel - 2s^2)}{\varepsilon_\parallel(\varepsilon_\parallel - s^2)^{1/2}}\theta - s\left(\frac{\varepsilon_\perp}{\varepsilon_\parallel}\right)^{1/2}\right\}. \tag{37}$$

Again, equation (37) can be considered as a torque balance equation, i.e. $\mathbf{\Gamma}_K + \mathbf{\Gamma}_{OPT} = 0$, where

$$\Gamma_{OPT} = H(\theta). \tag{38}$$

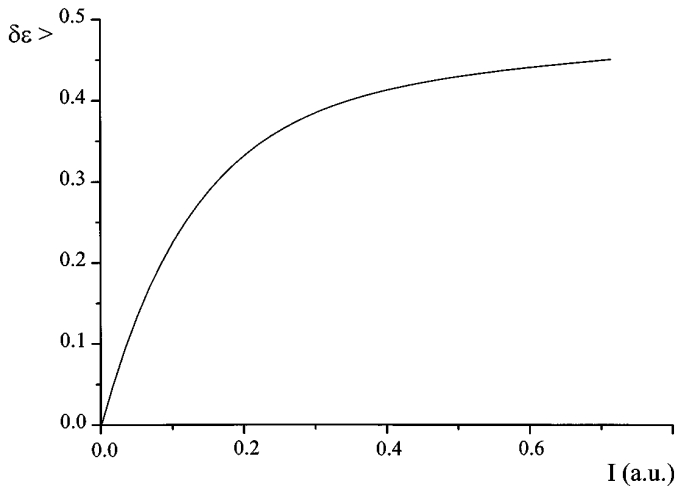

Figure 4. Average nonlinear dielectric permittivity of a hybrid aligned cell ($\theta_1 = 0$, $\theta_2 = \pi/2$) under strong anchoring conditions against the impinging light intensity I at normal incidence. The following parameters have been used: $d = 10$ μm; $K_a = 0.074$; $\varepsilon_\parallel = 3.2$; $\varepsilon_\perp = 2.4$.

Equation (37) has the simple solution:

$$\theta = A^2 \frac{\Delta\varepsilon}{16\pi K_3} \sin\beta_0 \left(\frac{\varepsilon_\perp}{\varepsilon_\parallel}\right)^{1/2} \left[z^2 - \left(\frac{d}{2}\right)^2\right]. \tag{39}$$

Under the approximation $\Delta\varepsilon/\varepsilon_\perp \ll 1$ and for small reorientations it is possible to write

$$\varepsilon_{eff} = \varepsilon_\perp[1 + (\Delta\varepsilon/\varepsilon_\parallel)\sin^2\beta + 2\theta(\Delta\varepsilon/\varepsilon_\parallel)\sin\beta\cos\beta] \tag{40}$$

where the last term

$$\delta\varepsilon = 2\Delta\varepsilon\theta(z)(\varepsilon_\perp/\varepsilon_\parallel)\sin\beta\cos\beta \tag{41}$$

represents the nonlinear part and β is the internal incidence angle. Averaging over the cell thickness d, one obtains

$$\langle\delta\varepsilon\rangle = A^2 \frac{\Delta\varepsilon^2}{8\pi K_3} \left(\frac{\varepsilon_\perp}{\varepsilon_\parallel}\right)^{3/2} \frac{d^2}{6} \sin\beta_0 \sin\beta\cos\beta. \tag{42}$$

As for the homeotropic cell the zero intensity refractive index is $n^0_{eff} \approx (\varepsilon_\perp)^{1/2}$ and $\sin\beta_0 \approx (\varepsilon_\parallel)^{1/2}\sin\beta$, considering the relation between A^2 and the light intensity I, the nonlinear part of the refractive index becomes:

$$\langle\delta n\rangle = \left[\frac{\Delta\varepsilon^2}{2K_3 c\varepsilon_\parallel} \left(\frac{\varepsilon_\perp}{\varepsilon_\parallel}\right)^{1/2} \frac{d^2}{6} \sin^2\beta\cos^2\beta\right] I. \tag{43}$$

According to the usual definition $n = n^0 + n_2 I$ we have then

$$n_2^{HOM} = \left[\frac{\Delta\varepsilon^2}{2K_3 c\varepsilon_\parallel} \left(\frac{\varepsilon_\perp}{\varepsilon_\parallel}\right)^{1/2} \frac{d^2}{6} \sin^2\beta\cos^2\beta\right]. \tag{44}$$

This final expression is very useful to point out the dependence of the nonlinear part of the refractive index on the materials parameters and on the geometry used. The most important feature related to the material properties is the dependence on the square of the

optical anisotropy $\Delta\varepsilon$, which accounts for the huge value of the obtained optical nonlinearity as consequence of the highly anisotropic properties of LCs. Using the parameters of the nematic liquid crystal E7 ($\varepsilon_\parallel = 3.01$, $\varepsilon_\perp = 2.33$, $\Delta\varepsilon = 0.68$, $K = 10^{-6}$ dynes) with $d = 50$ μm and $\beta = 15^\circ$ we obtain $n_2 = 0.5 \times 10^{-5}$ cm^2 W^{-1} which is a very high value if compared to conventional nonlinear liquids. At intensities of the order of 10^3 W cm^{-2}, an overall variation of the refractive index $\langle\delta n\rangle = 0.005$ can easily be obtained! It is interesting to underline that such a huge nonlinear response gives rise a strong nonlinear phase shift $\delta\psi = (2\pi/\lambda)\langle\delta n\rangle d$, given by:

$$\delta\psi_{NL}^{HOM} = \frac{2\pi}{\lambda} d\left[\frac{\Delta\varepsilon^2}{2K_3 c\varepsilon_\parallel}\left(\frac{\varepsilon_\perp}{\varepsilon_\parallel}\right)^{1/2}\frac{d^2}{6}\sin^2\beta\cos^2\beta\right]I. \tag{45}$$

Using the above parameters we obtain $\delta\psi = \pi$ at $\lambda = 514.5$ nm. Similar results can also be obtained starting with a different prealignment of the liquid crystal such as the planar or the hybrid one.

The huge nonlinear phase shift induced by the nonlinear response gives rise to the amazing ring pattern observed by focusing the light beam on the sample (figure 5). As pointed out above, it is quite easy to reach intensities that produce phase shifts of several π, so that the different parts of the beam corresponding to the same wavevector give rise to an interference pattern which is easily observable with liquid crystals. The maximum phase shift can be obtained by simply counting the overall number N of rings, i.e. $\delta\psi_{MAX} = N2\pi$ (figure 6).

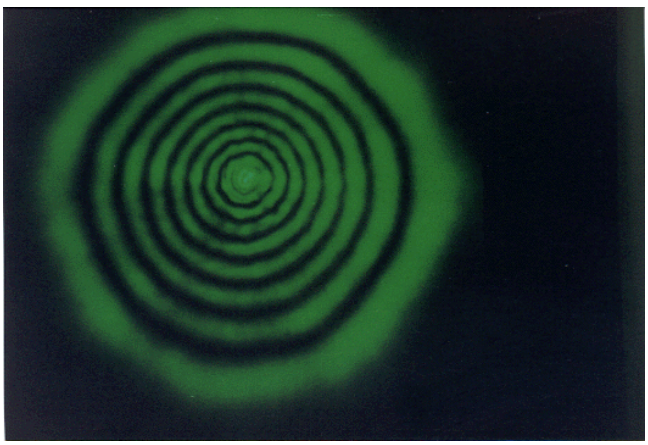

Figure 5. The amazing ring pattern due to self-phase modulation in liquid crystals.

2.4. Threshold effects

In the discussion on the optically induced torque we have considered a light beam impinging on a liquid crystal sample with an incidence angle $\beta_0 \neq 0$. On the other hand, the condition $\beta_0 = 0$ gives rise to important consequences.

Let us consider the optical torque for a polarized dielectric:

$$\boldsymbol{\Gamma}_{OPT} = (1/4\pi)(\boldsymbol{D} \times \boldsymbol{E}). \tag{46}$$

Using the expression of the electric induction for nematics

$$\boldsymbol{D} = \varepsilon_\perp \boldsymbol{E} + \Delta\varepsilon(\boldsymbol{n} \cdot \boldsymbol{E})\boldsymbol{n} \tag{47}$$

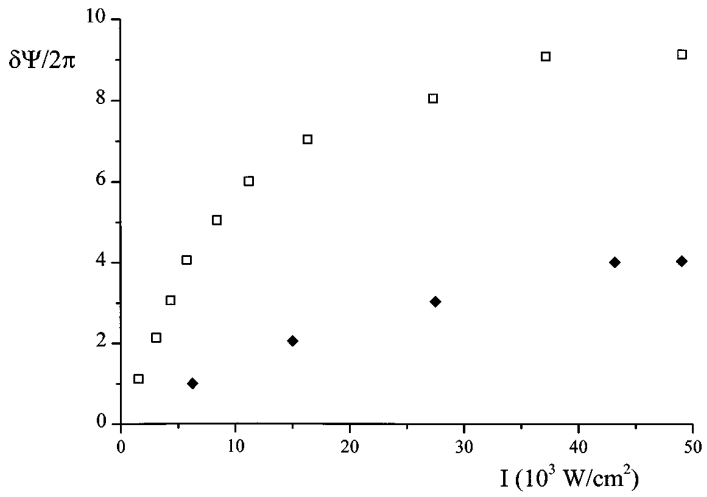

Figure 6. An example of the behaviour of the nonlinear optical phase shift against the impinging light in a pump–probe experiment. Upper data refer to a 50 μm thick sample, lower data to a 28 μm thick sample. (After Umeton *et al* [18].)

and considering a complex optical field, we obtain

$$\boldsymbol{\Gamma}_{OPT} = (\Delta\varepsilon/8\pi)(\boldsymbol{n}\cdot\boldsymbol{E}^*)(\boldsymbol{n}\times\boldsymbol{E}). \tag{48}$$

This expression allows us to point out that the optical torque is present only when the angle between the director and the optical field is different from $\pi/2$ and, obviously, from 0. However, the liquid crystal is an optically anisotropic (usually uniaxial) medium and an electromagnetic wave splits into two components, an ordinary and an extraordinary wave, when propagating through it. The ordinary wave always fulfils the condition $\boldsymbol{n}\cdot\boldsymbol{E} = 0$, therefore no optical torque can be originated from it. As a consequence, only the extraordinary wave can induce optical reorientation and then can be affected by it during the propagation, thus producing nonlinear optical effects. When a linearly polarized beam impinges upon a uniformly aligned homeotropic nematic sample at an incidence angle $\beta_0 = 0$, the wavevector is parallel to $\boldsymbol{n}$, then $\boldsymbol{\Gamma}_{OPT} = 0$ and no reorientation occurs. However, the thermal fluctuations of the molecules around the direction of $\boldsymbol{n}$ make possible a coupling with the optical field. In this case, if the intensity of the field becomes strong enough, the initial orientation becomes unstable and a reorientation may occur. As soon as a small reorientation is established, it can be continuously increased due to the appearance of an extraordinary wave in the medium. This is the typical configuration leading to the threshold phenomenon which in homeotropically aligned samples is called the optical Fredericksz transition (OFT). It is characterized by a well defined threshold intensity and may occur whenever the initial geometry allows propagation of only the ordinary wave. OFT is the optical counterpart of the well known Fredericksz transition effect induced by static magnetic or electric fields in LCs. The OFT and the other threshold phenomena can be considered as *order transition* effects and the possibility of driving this transition with a light beam may have important consequences. As a matter of fact, many different cases can be considered which cannot be treated in the same way, therefore we will give here a brief description of the OFT as the most important example of these effects.

Considering a linearly polarized beam impinging at normal incidence on a homeotropically aligned sample, near threshold the small distortion approximation is certainly fulfilled, so we

can use equation (36) with $s = 0$ taking into account that for small θ, $E_x = A(\varepsilon_\parallel)^{1/4}$; then

$$\frac{\mathrm{d}^2\theta}{\mathrm{d}z^2} + \frac{\Delta\varepsilon}{8\pi K_3}|E_x|^2\frac{\varepsilon_\perp}{\varepsilon_\parallel}\theta = 0. \tag{49}$$

This equation is very similar to the one obtained in the low frequency or static case where the field E replaces the term $\frac{1}{2}E_x(\varepsilon_\perp/\varepsilon_\parallel)$. The strong anchoring boundary conditions $\theta_1 = \theta_2 = 0$ make $\theta(z) = 0$ a stable solution throughout the whole cell. This solution becomes unstable when E_x exceeds a threshold value. This result is found from the time dependent Euler–Lagrange equation

$$\frac{\mathrm{d}^2\theta}{\mathrm{d}z^2} + \frac{\Delta\varepsilon}{8\pi K_3}|E_x|^2\frac{\varepsilon_\perp}{\varepsilon_\parallel}\theta = \frac{\gamma}{K_3}\frac{\partial\theta}{\partial t} \tag{50}$$

where γ is a viscosity coefficient. Looking for solutions in the form $\theta(z,t) = \sum\theta_q(t)\sin[(q\pi/d)z + \pi/2]$, each time-dependent amplitude function $\theta_q(t)$ is found to obey the following equation

$$-q^2\left(\frac{\pi}{d}\right)^2\theta_q + \frac{\Delta\varepsilon}{8\pi K_3}|E_x|^2\frac{\varepsilon_\perp}{\varepsilon_\parallel}\theta_q = \frac{\gamma}{K_3}\frac{\partial\theta_q}{\partial t} \tag{51}$$

whose solution is

$$\theta_q(t) = \theta_q(0)\,\mathrm{e}^{\Gamma_q t} \tag{52}$$

with

$$\Gamma_q = \frac{(\Delta\varepsilon/8\pi K_3)(\varepsilon_\perp/\varepsilon_\parallel)|E_x|^2 - q^2(\pi/d)^2}{\gamma/K_3}. \tag{53}$$

This solution becomes stable when $\Gamma_q > 0$, that is above a threshold field given by

$$E_{th} = \left(\frac{8\pi^3 K_3\varepsilon_\parallel}{\Delta\varepsilon d^2\varepsilon_\perp}\right)^{1/2} \tag{54}$$

which corresponds to a threshold in the intensity given by

$$I_{th} = \frac{cK_3}{\Delta\varepsilon}\frac{\varepsilon_\parallel}{\varepsilon_\perp^{1/2}}\frac{\pi^2}{d^2}. \tag{55}$$

Above threshold the director distribution is described by

$$\theta(z) = \theta_M\sin[(\pi z/d) + \pi/2] \tag{56}$$

where θ_M can be calculated from equation (49)

$$\theta_M \approx \left(\frac{I/I_{th} - 1}{4B}\right)^{1/2} \tag{57}$$

with B given by [31]

$$B = \frac{1}{4}\left(1 - K_a - \frac{9\Delta\varepsilon}{4\varepsilon_\parallel}\right). \tag{58}$$

The expression for θ_M points out the rapid increase of the distortion above threshold: it is easy to obtain reorientation of 30° with a light intensity of only 10% above the threshold value. It is worth just recalling that the OFT and similar phenomena can be dealt with using methods typical of phase-transition study (Landau–De Gennes expansions [29]); however, such an approach is well beyond the aim of this paper.

2.5. Effects of boundary conditions

A wider phenomenology of *order transitions* can be found when the strong anchoring condition is not fulfilled. In this case, Euler–Lagrange equations must be considered also for the boundaries. Under the hypothesis of planar reorientation, the free energy at the surfaces can be written as [28]

$$\begin{aligned} F_{s1}(\theta) &= (1/2)W_{s1}\sin^2(\theta - \theta_1^*) \\ F_{s2}(\theta) &= (1/2)W_{s2}\sin^2(\theta - \theta_2^*) \end{aligned} \tag{59}$$

and the following equations are finally obtained:

$$L_i\{[1 - K_a\sin^2\theta_i][c^2 - f(\theta_i, I)]\}^{1/2} = \pm\sin(\theta_i - \theta_i^*)\cos(\theta_i - \theta_i^*) \tag{60}$$

where θ_1^* and θ_2^* are the pretilt angles and W_i and $L_i = K_3/W_i$ ($i = 1, 2$) are the anchoring energies and the extrapolation lengths, respectively, corresponding to the two boundary surfaces. From a mathematical point of view the problem is now more complex as we have three unknown quantities θ_1, θ_2 and c^2 to be determined by simultaneous solution of equations (28) and (60). Once we have solved this system of equations, we can calculate the actual director distribution $\theta(z)$. In general we obtain an enhancement of the nonlinear reorientation, a result that is easy to understand since in this case also the molecules close to the boundaries can be reoriented thus strengthening the nonlinear response.

By coupling the equations for the boundary conditions with the Euler–Lagrange equations for the bulk, it is possible to study in a general way the stability of different configurations under different boundary conditions. In this way it is possible to work out a sort of phase diagram, called a *phase-order diagram*, where intensity is reported on one axis and sample thickness on the other one. An example [28] of such a diagram is given in figure 7, where d against I is plotted for a liquid crystal cell with $\theta_1^* = 0$ and $\theta_2^* = \pi/2$ (hybrid aligned nematic) and extrapolation lengths $L_1 = 1\ \mu$m, $L_2 = 5\ \mu$m. The meaning of this diagram is in the mapping of the I,d space into regions of stability for the different order configurations. The borderlines separating the different regions identify, for each sample thickness, the threshold intensity that is required to drive the transition from one order configuration to another one. In the case of figure 7, transitions from homeotropic to hybrid to planar order are possible. The diagram also shows when a nonlinear optical behaviour can be expected; in fact, only a distorted configuration gives rise to a nonlinear response. Therefore, with reference to figure 7, a nonlinear response in possible only in the HAN region.

2.6. Plane waves with elliptical polarization

We have already observed that in spite of the parallelism existing between the interaction of a liquid crystal with a low frequency field and its interaction with an optical field, a major qualitative difference is due to the constraints imposed to the fields by the Maxwell wave equation. However, for linearly polarized waves the equations obtained for the optical field may be very similar to those of the static case. In contrast, something completely new occurs when one considers light with elliptical polarization impinging on the liquid crystal sample. Santamato and coworkers have carried out extensive theoretical studies [32–34] and experimental investigations [35–39] on the effects of an elliptically polarized plane wave normally incident on a nematic liquid crystal, extending these studies to chiral nematics [40] and to smectic C* liquid crystals [41].

In this case we must consider a non-planar reorientation and represent the director as:

$$\boldsymbol{n} = \sin\theta\cos\phi\boldsymbol{x} + \sin\theta\sin\phi\boldsymbol{y} + \cos\theta\boldsymbol{z}. \tag{61}$$

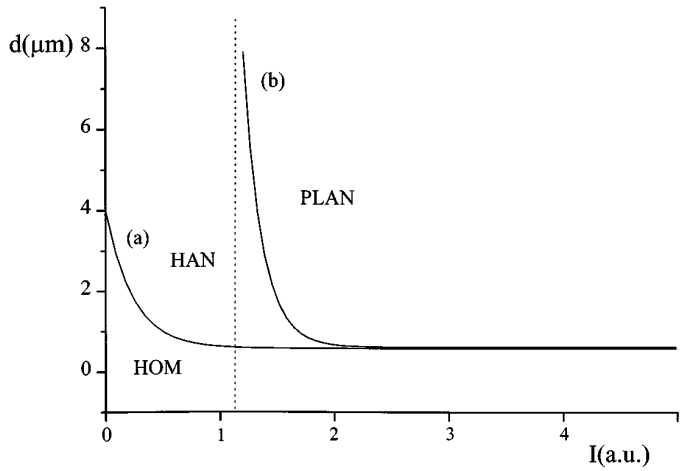

Figure 7. Sample thickness d against the intensity as obtained in the weak anchoring ($L_1 = 1\ \mu$m and $L_2 = 5\ \mu$m) for a HAN cell. The curves define the different regions of stability for the HOM, HAN and planar (PLAN) configuration. The following parameters have been used: $K_a = 0.074$; $\varepsilon_\parallel = 3.2$; $\varepsilon_\perp = 2.4$.

Keeping the plane wave approximation it is still possible to write $\theta = \theta(z)$ and $\phi = \phi(z)$, with $\partial/\partial x = \partial/\partial y = 0$. As a consequence the elastic free energy density becomes

$$F_K = \frac{1}{2}(K_1 \sin^2\theta + K_3 \cos^2\theta)\left(\frac{\mathrm{d}\theta}{\mathrm{d}z}\right)^2 + \frac{1}{2}(K_2 \sin^2\theta + K_3 \cos^2\theta)\sin^2\theta\left(\frac{\mathrm{d}\phi}{\mathrm{d}z}\right)^2 \tag{62}$$

Assuming negligible absorption (i.e. constant intensity throughout the cell) and in the framework of the GOA, the total electromagnetic energy density can be written as

$$w_E = (1/8\pi)(\boldsymbol{E}^o \cdot \boldsymbol{D}^o + \boldsymbol{E}^e \cdot \boldsymbol{D}^e) = (1/8\pi)(n_o^2|E^o|^2 + n(\theta)^2|E_\perp^e|^2) \tag{63}$$

where $\boldsymbol{E}_\perp^e = \boldsymbol{E}^e - \boldsymbol{z}(\boldsymbol{z} \cdot \boldsymbol{E}) = E_x \cos\phi + E_y \sin\phi$, and $n_o = n_\perp$.

In the low birefringence approximation $n(\theta) - n_o \ll 1$. Equation (63) can be rewritten in a more manageable form as

$$w_E = \frac{I}{c}n_o + \frac{I}{2c}[n(\theta) - n_o]\{1 + (1 - e^2)^{1/2}\cos[2(\psi - \phi)]\} \tag{64}$$

where e is the wave ellipticity and ψ is the angle between the ellipse major axis and the x axis. Then the total free energy density is written as $F = F_K - w_E$ and minimization is carried out. The following two equations are then obtained

$$\frac{\mathrm{d}}{\mathrm{d}z}\left[(K_2 \sin^2\theta + K_3 \cos^2\theta)\sin^2\theta\frac{\mathrm{d}\phi}{\mathrm{d}z}\right] + \frac{I}{c}[n(\theta) - n_o](1 - e^2)^{1/2}\sin[2(\psi - \phi)] = 0 \tag{65a}$$

$$\begin{aligned}[K_3 - (K_3 - K_1)\sin^2\theta]\frac{\mathrm{d}^2\theta}{\mathrm{d}z^2} - (K_3 - K_1)\sin\theta\cos\theta\left(\frac{\mathrm{d}\theta}{\mathrm{d}z}\right)^2 \\ - \sin\theta\cos\theta[K_3 - 2(K_3 - K_2)\sin^2\theta]\left(\frac{\mathrm{d}\phi}{\mathrm{d}z}\right)^2 \\ + \frac{I}{2c}\frac{\mathrm{d}n(\theta)}{\mathrm{d}\theta}\{1 + (1 - e^2)^{1/2}\cos[2(\psi - \phi)]\} = 0.\end{aligned} \tag{65b}$$

These equations must be solved together with those concerning the reduced Stokes parameters ($s_i = P_i/P$) which, under the GOA, obey a precession equation

$$\frac{\mathrm{d}\boldsymbol{s}}{\mathrm{d}z} = \boldsymbol{\Omega} \times \boldsymbol{s} \tag{66}$$

where P_i are the usual Stokes parameters and

$$\boldsymbol{\Omega} = (\omega/c)[n(\theta) - n_o](\cos 2\phi, \sin 2\phi, 0). \tag{67}$$

Writing equation (65*a*) in a different form it is possible to work out its fundamental meaning. It is well known that an elliptically polarized monochromatic wave carries an angular momentum given by:

$$L_z = (I/\omega)\sin 2\chi \tag{68}$$

with $P_3 = P_0 \sin 2\chi$. Taking into account the precession equation (66) we obtain

$$\frac{\mathrm{d}L_z}{\mathrm{d}z} = \frac{I}{c}[n(\theta) - n_o]\{(1-e^2)^{1/2}\sin[2(\psi - \phi)]\} \tag{69}$$

which compared to equation (65*a*) gives

$$\frac{\mathrm{d}}{\mathrm{d}z}\left[(K_2 \sin^2\theta + K_3\cos^2\theta)\sin^2\theta\frac{\mathrm{d}\phi}{\mathrm{d}z}\right] + \frac{\mathrm{d}L_z}{\mathrm{d}z} = 0. \tag{70}$$

This equation is nothing else than the conservation law of angular momentum. The first term in square brackets is the angular momentum that is transferred to the liquid crystal from the light losing angular momentum according to the derivative $\mathrm{d}L_z/\mathrm{d}z$; whenever $\mathrm{d}\phi/\mathrm{d}z \neq 0$ an exchange of angular momentum takes place.

Equation (65) can be applied to the very important case of a purely twisted liquid crystal where θ = constant and $\phi = \phi(z)$; this situation occurs both in twisted nematics and in smectic C*. In this case the two equations become

$$\frac{C}{2}\left(\frac{\mathrm{d}\phi}{\mathrm{d}z}\right)^2 + \frac{I}{c}\left[n_o + \frac{n(\theta) - n_o}{2}\right]\{1 + (1-e^2)^{1/2}\cos[2(\psi-\phi)]\} = E = \text{constant} \tag{71a}$$

$$C\left(\frac{\mathrm{d}\phi}{\mathrm{d}z}\right) + \left(\frac{I}{\omega}\right)e = M = \text{constant} \tag{71b}$$

where $C = (K_2\sin^2\theta + K_3\cos^2\theta)\sin^2\theta$. Eliminating $\mathrm{d}\phi/\mathrm{d}z$ between them, E can be calculated

$$E = \frac{I}{c}\left[n_o + \frac{n(\theta) - n_o}{2}\right] + \frac{1}{2C}\left(M - \frac{Ie}{\omega}\right)^2 + \left(I\frac{n(\theta) - n_o}{2c}\right)(1-e^2)^{1/2}\cos[2(\psi-\phi)] \tag{72}$$

and accordingly

$$\left(\frac{\mathrm{d}e}{\mathrm{d}z}\right)^2 = \left[\frac{\omega}{c}(n(\theta) - n_o)\right]^2(1-e^2) - \left[E - \left(\frac{I}{c}\right)\left(n_o + \frac{n(\theta)-n_o}{2}\right) - \left(\frac{1}{2C}\right)\left(M - \frac{Ie}{\omega}\right)^2\right]^2\left(\frac{2\omega}{I}\right)^2. \tag{73}$$

This equation can be solved in terms of elliptic integrals, and the constants M and E are determined by the boundary conditions.

Equations (72) and (73) are the starting point to study the effects of the optical torque on twisted structures, one example being the OFT in twisted nematics. However, little experimental work has been done on this subject up to now. In contrast, the most amazing

results have been obtained when considering the dynamic behaviour. Different dynamic regimes have been demonstrated [37]: distorted equilibrium states, persistent oscillations and precession–nutation regimes. Spontaneous and peculiar routes to chaotic oscillations have also been observed [42].

In order to understand how the angular momentum transfer can be linked to the director motion it is necessary to consider again the time dependent Euler–Lagrange equations. To this purpose the dissipative function is identified with the viscous torque. In this case, the angular momentum conservation law integrated over the cell thickness is written as

$$\gamma \int_0^d \left(\frac{\partial \phi}{\partial t}\right) \sin^2 \theta \, \mathrm{d}z = \frac{I}{\omega} \Delta s_3 \tag{74}$$

where Δs_3 is the variation of the ellipticity between the exit and the entrance plane. Since Δs_3 is proportional to the variation of angular momentum it means that this variation induces a precession of the director around the z axis. In this way, depending on the polarization state of the impinging light, on the light intensity and on the pretilt angles, different combination of distortion (distributions $\theta(z)$) and azimuthal motion ($\phi(t)$) may be present, which explain the different dynamical regimes experimentally observed.

2.7. The Jánossy effect

Since 1990 Jánossy and coworkers have reported [43–48] an anomalous behaviour in a dye-doped nematic liquid crystal submitted to optical fields. They discovered that in homeotropic samples of guest–host mixture (dye concentration 1–2%) the threshold for the optical Fredericksz transition was two orders of magnitude lower than in pure nematics, it being possible to induce it with pump powers of 1 mW or less. After some experiments it became clear that a thermomechanical coupling due to heating of the sample could not explain the observations since different dyes having the same absorption coefficient gave rise to different behaviours. In particular, while anthraquinone dyes produced the effect, azo-dyes did not. This fact revealed that laser heating could not be responsible for low power reorientations. Moreover, the experimental observations were in complete agreement with the above described phenomenology that is typical of an optical torque acting on the liquid crystal. On the other hand, the low concentration of dyes in the mixture only slightly affects the material parameters such as Δn or K and this cannot account for the huge change in the optical power necessary to induce the reorientation. For all these reasons, the first step made in order to explain this effect was to consider an additional light-induced torque superimposed on the usual optical torque. Then, based on the similarity between the behaviour observed in doped and pure nematics, the additional torque could be written as:

$$\boldsymbol{\Gamma}_{DYE} = \eta \boldsymbol{\Gamma}_{OPT} \tag{75}$$

η being a parameter characteristic of the dye. The observed decrease of the threshold of OFT by two orders of magnitude indicates a value of η of about 100. By introducing a dimensionless parameter $\zeta = \eta \Delta\varepsilon$, which depends only on the structure of the particular dye, it is possible to write

$$\boldsymbol{\Gamma}_{DYE} = (\zeta/8\pi)(\boldsymbol{n} \cdot \boldsymbol{E}^*)(\boldsymbol{n} \times \boldsymbol{E}). \tag{76}$$

As a matter of fact, a more extended experimental investigation has shown that ζ may have positive or negative values, depending on the structure of the dye.

The Jánossy effect has been probably the first of a series of several different phenomena observed in guest–host systems where the orientation of the director is strongly affected by the light. It is still an open question whether a number or most of these phenomena are nothing

else than different aspects of a general type of interaction occurring between dye and liquid crystal molecules. We mention here the Jánossy effect because from a macroscopic point of view it appears just as an enhancement of the optical torque even though its microscopic origin seems to be much more complex. In contrast, the effects related to phototransformation of the dye molecules, such as photoisomerization, will be discussed later.

The basic assumption made for explaining the anomalous reorientation is the existence of a peculiar interaction between the excited dye molecules and the liquid crystal. In particular, it is assumed that the mean field acting on the dye molecules is different in the ground state and in the excited state.

Marrucci and Paparo [49] have recently developed a microscopic model where they consider the additional photoinduced torque due to light absorption by the dye molecules as distinct from the optical (or electromagnetic) torque as defined above. Through a balance of all the average torques acting on all the molecules, they find that the photoinduced torque must be interpreted as a friction torque. This friction corresponds to an angular momentum transfer between a rotating molecule and its neighbour molecules due to intermolecular interactions. In the limit of small dye anisotropy and small light intensity they were able to find an approximate expression for the photoinduced torque parameter ζ

$$\zeta = \frac{16\pi}{15}\sigma N_d S \frac{\tau_e N_h}{1 + 6D_e\tau_e}\left(u_{eh} - \frac{D_e}{D_g}u_{gh}\right). \tag{77}$$

Here S is the host order parameter, u_{eh} and u_{gh} are coefficients which describe the strength of the dye–host orientational interaction, D_e and D_g are the rotational diffusion constants in the excited and in the ground state, respectively, τ_e is the lifetime of the excited level, N_d and N_h are the total number of dye and host molecules per unit volume and σ the absorption cross section. The expression (77) is useful to identify the most important parameters affecting the Jánossy effect. The first one is σN_d which can be easily related to the absorption coefficients for the extraordinary and ordinary waves

$$\sigma N_d = \frac{c(n_e\alpha_e + 2n_o\alpha_o)}{8\pi h\nu}. \tag{78}$$

Another parameter is the decay time of the non-equilibrium dye distribution

$$\tau_d = \frac{\tau_e}{1 + 6D_e\tau_e}. \tag{79}$$

A third important parameter Δu takes into account the change occurring in the intermolecular interactions of a dye molecule with its environment when it is electronically excited

$$\Delta u = \left[u_{eh} - u_{gh}\left(\frac{D_e}{D_g}\right)\right]N_h. \tag{80}$$

It depends on the mean field change and on the variation of diffusion coefficients. This parameter is actually the most sensitive to the molecular structure of both the dye guest and the nematic host. Reasonable values of the model parameters such as $\Delta u = 0.1$ eV, $\tau_d = 10^{-9}$ s and $\alpha = 100$ cm^{-1} give a value of $\zeta = 100$, in agreement with the experimental findings in the most effective dye–LC mixtures.

3. Photoisomerization

3.1. General aspects of the phenomenon

Polarized light can exert a torque on the director of a nematic LC via interaction with light-absorbing azo-dye molecules (i.e. molecules containing the azo group) dissolved in the LC

matrix. This effect is due to a photoinduced conformational change of the azo-dyes, which is called photoisomerization.

Light-induced isomerization of azobenzene derivatives is a well known phenomenon that has been extensively studied in the past [50]. Azobenzene derivatives may exist as two geometric isomers, the *trans* and the *cis* form. These two configurations differ in the direction of the central bonds (figure 8). In the energetically more stable *trans* state the two bonds linking the azo group to the aromatic rings are parallel, resulting in an elongated shape of the molecule. In the metastable *cis* state the angle between the two bonds is 120 degrees and the molecules adopt a V-like conformation. The two isomers differ in their absorption spectra. In addition, their orientational orders in nematic LCs are different too, namely the *trans* form is significantly more ordered than the *cis* one. The mechanism of the *trans–cis* isomerization process is schematically represented in figure 9. The photoisomerization reaction begins by elevation of molecules to electronically excited states, followed by nonradiative decay back to the ground state in either the *cis* or *trans* form. This latter process involves a sequence of steps including (i) relaxation of the nuclear coordinates towards the energy minimum, (ii) de-excitation and (iii) further relaxation leading to one of the two isomeric forms. The absorption spectra of *trans*-azobenzenes exhibit their absorption maxima at around 350 nm due to a π–π^* transition and at around 450 nm due to an n–π^* transition. The *trans–cis* isomerization is a reversible process and the *trans* form is regenerated by exposure to visible light of the proper wavelength (around 440 nm). The ratio of *cis*/*trans* states is dependent on the quantum yield of the appropriate photoisomerization reaction (ϕ_{TC} and ϕ_{CT} for the *trans–cis* and the reverse *cis–trans* photoisomerization reactions, respectively). As the *trans* isomer is generally more stable than the *cis* isomer (for azobenzenes the energy barrier at room temperature is approximately 50 kJ mol^{-1}), molecules in the *cis* form may convert to the *trans* form by one of two mechanisms: (1) a spontaneous thermal back reaction, or (2) a reverse *cis* $\rightarrow$ *trans* photoisomerization cycle. The *trans–cis* equilibrium can be controlled through the wavelength and the polarization of the irradiating light [50]. The sensitivity of the photoisomerization reaction to the light polarization originates from the highly anisotropic shape of the azo-dye molecules in the *trans* form. Indeed, as the transition dipole moment of the azo-dye molecule is directed along its long principal axis, the probability of an azo unit's absorbing a photon and subsequently isomerizing is proportional to the cosine square of the angle between the transition dipole moment and the polarization direction of the exciting light. The molecules aligned parallel to the polarization of the exciting light, therefore, have the highest probability of being excited and isomerized. Consequently, when starting from isotropically distributed *trans* isomers, linearly polarized green light burns a hole in this angular distribution because of the selectivity of the molecular excitation and the concomitant *trans–cis* isomerization. This process is called *orientational hole burning*. Furthermore the principal axis of the molecule is reoriented as a result of the isomerization reaction (orientational redistribution). Because of orientational hole burning and orientational redistribution, *trans* molecules leave the direction parallel to the pump polarization and eventually align perpendicular to this direction.

Photoisomerization-induced molecular reorientation, accompanied often by strong photoinduced dichroism and optical anisotropy, has been observed in viscous solutions, amorphous and LC polymers, low molecular weight liquid crystals and Langmuir–Blodgett films [51]. However, its physical mechanism is not completely understood yet, although it is clear that the phenomenon is based on a photoselection of molecular oscillators whose transition moments coincide with the light polarization vector. Measurements of the light-induced dichroism accompanying the molecular reorientation in several guest–host systems showed that, after irradiation, the electronic oscillators of the dye are oriented perpendicularly to the

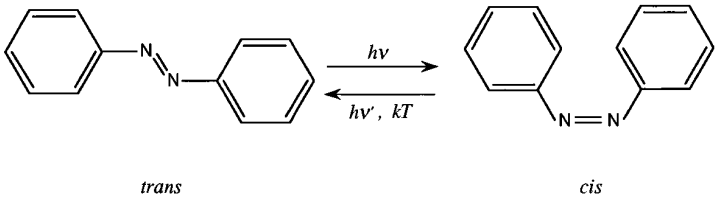

Figure 8. *Trans–cis* isomerization of azobenzenes.

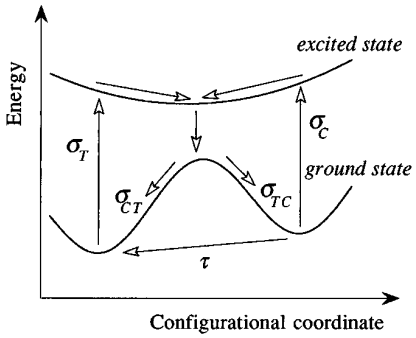

Figure 9. Schematic representation of the *trans–cis* isomerization process. σ_T and σ_C are the cross sections for absorption of one photon by a molecule in the *trans* or the *cis* state, respectively. Φ_{TC} and Φ_{CT} are the quantum yields of the transitions; they represent the probability per absorbed photon of the photochemical conversion. τ is the thermal relaxation rate for the *cis–trans* transition. This picture represents only simplified model of the molecular states. In fact, several excited states may be involved in the process whereas the nuclear motions cannot be represented in general with a single configurational coordinate.

light electric vector. It looks as if the electric vector repels electronic oscillators. Therefore the light absorbed within an electronic band of a dye exerts a torque on the dye molecules. If the same dye is incorporated in a nematic LC, the torque is transferred from the dye to the director of the LC. In the recent years, interesting applications of the photoinduced isomerization of azobenzenes have been proposed, such as data storage and holographic recording [52, 53], materials processing for second order NLO applications [54] and regulation of surface alignment in LC cells [55, 56]. In all these applications the dye molecules are embedded in a solid matrix which strongly limits their orientational mobility. Reorientation processes become possible, however, during the light-induced *trans–cis* or *cis–trans* transitions. In this way, light irradiation leads to a non-equilibrium orientational distribution of the dye molecules and a quadrupolar or even a polar order can be generated in the sample [57]. The reversible light-induced dichroism of azodyes (guests) in an amorphous polymer matrix (host) was studied in detail by Todorov *et al* [58]. The pump and probe technique was used to measure the changes in absorbances of dye molecules simultaneously with their optical excitation in the electronic band, corresponding to the π–π^* transition of the *trans* form. The measured decrease of the absorbance for probe polarization parallel to that of the pump and increase of the absorbance for perpendicular probe polarization confirmed the mechanism of molecular reorientation mediated by the *trans–cis* photoisomerization. The photoinduced dichroism was shown to be accompanied by a photoinduced optical anisotropy (birefringence) which enabled polarization holographic recording with high diffraction efficiency.

Very interesting papers have recently been devoted to the photoinduced anisotropy in amorphous polymer films [53, 59]. The key point is that the amorphous phase was prepared by rapid cooling from the isotropic phase of mesomorphic polymers and therefore it is metastable. If the system were cooled slowly the final state would be a nematic-like glass. In particular, Läsker *et al* [59] studied the UV and IR dichroism of a copolymer containing two pendent groups, an azobenzene chromophore and a dipolar rigid cyanobiphenyl fragment. Before excitation the angular distribution of the electronic oscillators of the chromophore and the vibrational oscillators of the cyanogroup were isotropic. On photoexcitation, they observed the electronic oscillators of the azobenzene chromophore to orient perpendicularly to the light electric vector, as expected for the *trans–cis* photoisomerization process. A result of particular relevance is the simultaneous reorientation of the photoelectrically inactive biphenyl moiety which, in fact, is driven to the new orientational state by its neighbour, i.e. the azobenzene chromophore. The photoinduced molecular reorientation in amorphous polymers may be easily modelled if one assumes an anisotropic photoselection of dye oscillators and free rotation of the photoexcited chromophores [60].

3.2. Photoisomerization in polymeric LCs

Polymer LCs can be studied in both a liquid crystalline and a glassy state and, in these two cases, the process of photoinduced molecular reorientation proceeds differently. Consider first the nematic LC phase. As is well known, LCs are characterized by a certain degree of orientational order that is quantitatively expressed by a quadrupolar order parameter tensor. This latter can be decomposed [29] into a scalar order parameter S and a unit vector of the preferential orientation of their molecular axes, the director $\boldsymbol{n}$. The scalar order parameter describes the amount of orientational order of the molecules with respect to the preferable direction $\boldsymbol{n}$, and is defined as [29]

$$S = \frac{1}{2}\langle(\cos^2\theta - 1)\rangle = \int_\Omega f(\theta)[(3\cos^2\theta - 1)/2]\,\mathrm{d}\Omega \tag{81}$$

where θ is the angle between the long molecular axis and the director $\boldsymbol{n}$, $f(\theta)$ is the orientational distribution function and $\mathrm{d}\Omega = \sin\theta\,\mathrm{d}\theta\,\mathrm{d}\phi$ is the solid angle. This parameter varies between $S = 0$ in the isotropic phase (when the random molecular orientation makes $f(\theta)$ independent of θ) and $S = 1$ when all the molecules are perfectly aligned in the same direction ($\theta = 0$ or $\theta = \pi$). The photoinduced anisotropy is quantitatively estimated by the orientational order parameter and can be calculated according to the usual definition as

$$S = \frac{\alpha_\parallel - \alpha_\perp}{2\alpha_\perp + \alpha_\parallel} \tag{82}$$

where $\alpha_\parallel$ and $\alpha_\perp$ are the absorption coefficients (or absorbances) for polarization direction parallel and perpendicular to the director, respectively (a detailed description of the relation between dichroism and order parameter is given in [61]).

A number of LC copolymers have been synthesized which contain azobenzene chromophores as pendent groups. The light absorbed by azobenzene chromophores causes the reversible *trans–cis–trans* isomerization of the azo-bridge as discussed above. Since the *cis*-form is not as elongated as the *trans*-form it decreases the order parameter and reduces the thermal stability of the nematic phase. The steady-state irradiation of a polymer in the nematic phase by polarized light results in reorientation of both the chromophore and neighbour mesogenic groups (and hence the nematic director) through the same angle in the direction outward of the light electric vector. This was verified by means of UV and IR polarization spectroscopy on a sample (see figure 10) frozen to room temperature just after irradiation [62].

The sample consisted of a nematic side chain co-polymer with one azo co-monomer being sensitive to light and the other being unable either to absorb light of the desired wavelength or to perform an isomerization upon irradiation. *In situ* kinetic measurements performed with the pump and probe technique allowed us to measure the lifetime of the photoinduced rise of birefringence [63]. Values variable in the range 20–60 s were found, independent of the phase state (nematic, smectic, even glassy). This means that the kinetics of the process is controlled by a kind of nonequilibrium (dynamic) microscopic viscosity. In contrast, relaxation times of the induced birefringence are found to be very long in the glassy state (hours) but rather short (minutes) in the nematic and smectic A phases.

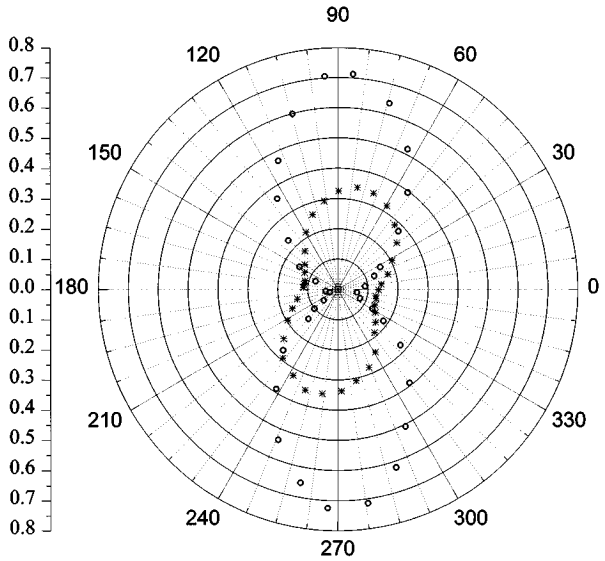

Figure 10. UV absorption diagram of the copolymer studied in [62], measured at 360 nm before (○) and after (∗) irradiation with polarized light of 488.0 nm. The absorption is reported as a function of the polarization of the measuring light. The direction of the irradiating light was tilted 10° with respect to the director. (After Anderle *et al* [62].)

It is of interest that in the glassy nematic state of a polymer studied in [62] there was no appreciable reorientation of cyanobiphenyl moieties driven by reorienting chromophores. This happens because the collective motion mentioned strongly depends on the molecular structure of polymers. Polarized light leads to an effective reorientation of the optic axis even in the glassy state of LC polymers containing the azobenzene mesogenic group, via the *trans–cis–trans* isomerization. This process is, in principle, based on a combination of a photoselection and a subsequent more or less random reorientational motion of the selected molecules as controlled by the local dynamics of the glassy state. A phenomenological description of this effect has been proposed [53, 64] which is able to account for the phenomena found for LC systems as well as for amorphous systems in the glassy state, and which allows one to calculate also changes of the orientational distribution far from the original one. The model is based upon the following assumptions: (a) a chromophore which is subjected to an isomerization cycle changes its direction within the glassy state more or less randomly due to the variation of its geometric shape from a stretched to a bent configuration; (b) the reorientation is the effect of the local mobility within the glassy state as controlled by free volume fluctuations

and of a partial or complete memory loss of the molecules undergoing an isomerization cycle as far as their original orientation is concerned; (c) the azobenzene molecules are held in the glassy matrix (there is no Brownian motion or any other effect which drives the molecules back to their original orientation distribution after having changed their orientation under the influence of an isomerization process); (d) the molecules are continuously subjected to the isomerization cycle during irradiation and the corresponding reorientational motions unless the transition dipole moment is perpendicular to the polarization direction of the light. The final state of orientation is one in which all chromophores fulfil this requirement. The relevant equations for photostationary systems in the melt or in solution are then

$$\begin{aligned}\frac{\mathrm{d[A]}}{\mathrm{d}t} &= \frac{I_{abs}^{tot}}{E_{tot}} d\{\Phi_{BA}\varepsilon_B[\mathrm{B}] - \Phi_{AB}\varepsilon_A[\mathrm{A}]\} \\ \frac{\mathrm{d[B]}}{\mathrm{d}t} &= \frac{I_{abs}^{tot}}{E_{tot}} d\{\Phi_{AB}\varepsilon_B[\mathrm{A}] - \Phi_{BA}\varepsilon_B[\mathrm{B}]\}\end{aligned} \tag{83}$$

where [A], [B] are the concentrations of the species A and B, ε_A, ε_B are the molar extinction coefficients, Φ_{AB}, Φ_{BA} are the respective quantum yields and E_{tot} is the total extinction for a cell with a thickness d. These equations can be extended to the solid state if the following assumptions are made: (1) in the solid state the concentration has to be replaced by the orientational distribution functions $f_A(\Omega)$ and $f_B(\Omega)$ which represent the concentration of molecules for every distinct solid angle; (2) the molecular extinction is replaced by the square of the product of the transition dipole moment and the vector of polarization; (3) the rotational diffusion step is represented by a transfer function $F_{AB}(\Omega, \Omega')$ which gives the probability for a molecule of pointing into Ω after a reaction, provided its initial orientation was given by Ω'. The total change of the orientation distribution function is then given by the integral over all Ω' which turn into Ω, multiplied by the rate of reacting molecules. The result is then [64]

$$\begin{aligned}\frac{\mathrm{d}}{\mathrm{d}t} f_A(\Omega) = &\frac{I_{abs}^{tot}}{E_{tot}} d\Bigg[\Phi_{BA}\int_{\Omega'} F_{BA}(\Omega', \Omega) f_B(\Omega')(M_B(\Omega')\boldsymbol{e}_\varphi)^2 \,\mathrm{d}\Omega' \\ &- \varphi_{AB}(M_A(\Omega')\boldsymbol{e}_\varphi)^2 f_A(\Omega)\Bigg] \\ \frac{\mathrm{d}}{\mathrm{d}t} f_B(\Omega) = &\frac{I_{abs}^{tot}}{E_{tot}} d\Bigg[\Phi_{AB}\int_{\Omega'} F_{BA}(\Omega', \Omega) f_A(\Omega')(M_A(\Omega')\boldsymbol{e}_\varphi)^2 \,\mathrm{d}\Omega' \\ &- \varphi_{BA}(M_A(\Omega')\boldsymbol{e}_\varphi)^2 f_B(\Omega)\Bigg].\end{aligned} \tag{84}$$

It is apparent that one stationary solution exists which corresponds to an orientation distribution function where all molecules are perpendicular to the initial vector of polarization, as experimentally observed. In addition, the model allows one to find a dynamic solution once one has selected an appropriate transfer function F_{AB}. With a Gaussian choice [53, 64]

$$F_{AB}(\Delta\xi) = A\,\mathrm{e}^{-n\sin^2(\Delta\xi)} \tag{85}$$

where n represents something like the rigidity of the matrix (a perfectly rigid matrix, $n = \infty$, reorients the dye molecules always back to the original distribution whereas a completely soft matrix, $n = 0$, does not give rise to any effective restoring force) one finds that the predictions of the rate equation agree quite well with the experimental results. The examples of time development of the reorientation of the optical axis in a side chain LC polymer reported in [53] also point out that side chain LC polymers can typically be characterized as rather soft materials.

The experimental results of Wendorff and coworkers [53, 64, 65] clearly indicate that polarized light leads to an effective reorientation of the optic axis in the glassy-state of LC side

chain polymers containing the azobenzene mesogenic group, via the *trans–cis* isomerization. In particular, upon irradiation in the glassy state only those molecules can change their reorientation which are isomerized by the incident light (see figure 11(a)). Furthermore their results indicate that the reorientation process in those systems is totally a local process if the irradiation is performed in the glassy state. Since there is no coupling of a selected molecule to the surroundings, it should be possible in principle to address the system on a molecular level, i.e. a single molecule. Another interesting experimental result which is predicted by the above simple phenomenological theory is the finding that the magnitude of reorientation depends only on the energy brought into the system by the incident light and not on its intensity. Differently from the glassy state, the experimental results performed illuminating the sample above the glass transition, i.e. in the nematic fluid state, revealed that upon irradiation in the viscous nematic state both the dye molecules as well as their surroundings can change their orientation (figure 11(b)). Thus, while it should be able to address single molecules in the glassy state, there is a collective process in the fluid nematic state, when photoselected rotational diffusion in an LC side chain polymer takes place.

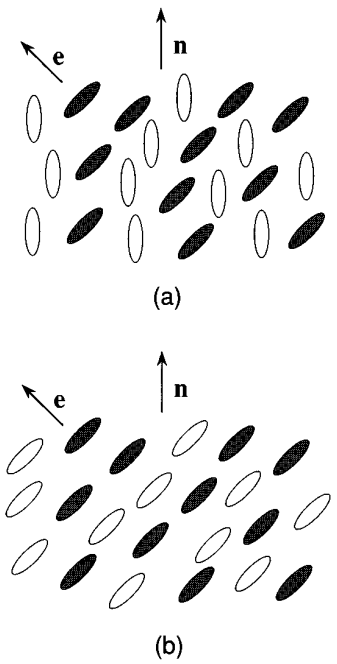

Figure 11. Schematic picture of the optical storage process on a molecular scale in a copolymer: (a) in the glassy state; (b) in the fluid nematic state. $\boldsymbol{n}$ is the initial director.

3.3. Photoisomerization in low molar mass LCs

Photoinduced conformational changes in conventional (low molar mass) liquid crystals containing azobenzene derivatives have been studied by a number of authors [66–69]. Particular interest has been paid to the photochemically induced switching of LC alignment at macroscopic scales in relation to potential applicability in displaying and processing the optical information. The applications of the *trans–cis* isomerization process involving photoinduced

(macroscopic) reorientation of the nematic director in LCs can be roughly divided into two categories, depending on whether the azo-dye molecules are incorporated over the surface of a solid polymeric layer [70–74] or on the contrary are dissolved within the LC host [75–85]. In the former case, photoinduced isomerization of azo-dyes has been used to realize the optically controlled alignment of LCs by means of 'command surfaces'. The first [55] example of this type of LC photoregulation was a reversible out-of-plane alignment alteration between homeotropic (perpendicular) and planar (parallel) modes using molecular layers of an azobenzene derivative upon alternate irradiation with UV (figure 12) and visible light for the reversible isomerization. In these systems, the photoactive surface molecules play the role of 'commander molecules' which control the alignment of the LC 'soldier molecules'. As an extension of the work on this type of alignment, Ichimura and coworkers reported the azimuthal (in-plane) reorientation of LC molecules induced by exposing an LC cell to linearly polarized UV light for the *trans–cis* photoisomerization and linearly polarized visible light for the *cis–trans* reverse process [71]. A closely related phenomenon of surface-mediated alignment induced by polarized light was found independently by Gibbons *et al* [70] who employed a polyimide doped with a dichroic azo-dye for a photoactive layer. They assembled a cell using this coated glass surface as the top plate and a second glass substrate, coated only with polyimide, as the bottom plate, both plates being mechanically rubbed to provide initial planar alignment of the LC. Within the illuminated region, the light-induced transformation of the photosensitive molecules resulted in the surface alignment of the LC director perpendicular to the polarization of the impinging light, whereas molecules adjacent to the undoped layer remained aligned parallel to the rubbing direction. Thus, the LC molecules in the cell assumed a twisted nematic structure within the illuminated region.

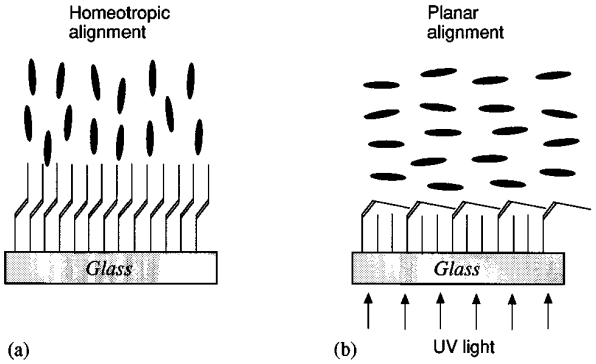

Figure 12. Principle of operation of a photoswitchable command surface for the control of the orientation of a liquid crystal. The molecular layer over the glass plate is an azobenzene derivative which undergoes the *trans–cis* photoisomerization when irradiated by UV light, thereby controlling the alignment of molecules in the overlying LC phase. The *trans–cis* isomerization is a reversible process and the *trans* form is regenerated by exposure to blue light.

The situation when the azo-dye molecules are dissolved in conventional liquid crystals to form guest–host systems is very different from that in solid films. In fact, conventional thermotropic LCs have low viscosity and short molecular relaxation times. Therefore, in these systems the dye molecules have a higher orientational mobility, a typical rotational relaxation time being of the order of nanoseconds. In addition one can only observe a reversible reorientation during steady-state irradiation. We have already seen that because of the orientational hole burning and orientational redistribution consequent to the isomerization

process, *trans* molecules leave the direction parallel to the pump polarization and eventually align perpendicular to this direction. In these systems such an effect generates a torque on the host-surrounding LC, which drags the LC molecules in the reorientation process and results in a collective molecular rotation until the long axis (hence the director $\boldsymbol{n}$) becomes perpendicular to the incident polarization. In other words, the light-induced torque is transferred from the dye to the director of the LC. In fact such a torque has already been observed in several experiments [46, 75, 80, 84–88]. In [75] the authors describe the alignment of a guest–host LC medium by means of polarized light. An LC cell was made from two glass substrates coated with a thin layer of polyimide. Both plates were rubbed prior to assembly and then assembled with the rubbing directions parallel. The cell was then filled with a dye–LC mixture of 1.8 wt% tetraazoperimedine dye in a commercial nematic LC at room temperature. The guest–host LC cell was then illuminated with an argon ion laser polarized parallel to the direction of the rubbing axis. After few minutes of exposure at 8 W cm^{-2} the LC in the illuminated region oriented perpendicular to the laser polarization and remained aligned in the absence of laser radiation.

The surface reorientation effects of the LC director, driven by the photoinduced bulk torque in an azo-dye doped LC cell has been first studied by Reznikov and coworkers [81]. They used a planar aligned LC cell where one boundary surface was coated by a polymeric layer providing a negligibly small azimuthal anchoring energy. The observed surface reorientation in the direction outward of the exciting light electric vector was attributed to the bulk director reorientation consequent to the *trans–cis* isomerization of the azo-dye molecules.

In spite of all the experimental observations, no physical model has yet been proposed which provides a complete analytical description of the light-induced torque in terms of the fundamental quantities involved in the process. The first quantitative analysis of the light-induced torque exerted on the director of a nematic LC from dye molecules was reported by Blinov *et al* [80]. The sign and magnitude of the torque were estimated from measurements of the light-induced dichroism using a pump–probe technique. Two guest–host systems were studied, both of them constituted of nematic mixtures with positive dielectric and optical anisotropy. A small amount of a dye was dissolved in each of the mixtures. One of them, an azo-anthraquinone, has an absorption band in the range 500–700 nm with a maximum at 670 nm, and a direction of the transition moment coinciding with the longitudinal molecular axis. In the LC matrix it exhibits positive dichroism, i.e. its absorbance for light with electric vector parallel to the director is higher than that for the perpendicular direction. The other dye, a biphenyl-anthraquinone dye, does not contain the azobenzene bridge and has an absorption maximum at 560 nm. The direction of its transient dipole moment is almost perpendicular to the longitudinal molecular axis and it is negatively dichroic. In the field-off planar state the light-induced dichroism was shown to be due only to the thermally induced decrease of the orientational order parameter, for both samples and any probe polarization. The situation changed dramatically when the initial planar orientation was disturbed by an ac external electric field (field-on regime) exceeding the Fredericksz transition threshold. In this situation, an additional photoinduced torque exerted on the director and directed outward from the light electric vector could be observed only for the mixture containing azo-dye. As an example, figure 13 shows the voltage-induced decrease in the absorbance of the probe beam (curve 1) and the change in the photoinduced absorbance (curve 2) measured with the azo-dye-doped sample planarly aligned along the vertical axis and with the probe and pump polarization at $\phi = 45^{\circ}$ and $\beta = -45^{\circ}$, respectively, to the vertical axis. The polarization dependencies of the photoinduced dichroism in the field-on regime clearly indicate that the azo-dye oscillators are deviated outward from the pump beam electric vector. The kinetics of this deviation corresponds to the director reorientation time and is found to be of the order

of 100–200 ms. The director is deviated in the same direction as the dye molecules, that is out of the exciting polarization. The authors observed [80] this kind of deviation of the rod-like dyes over the whole range of voltages above the Fredericksz transition threshold. Thus, the sign of the photoinduced torque exerted on dyes and the director in the absorbing LC under study is opposite to the sign of the torque exerted on the director of optically active positive LCs by the field of the light wave, for example in the case of the optical Fredericksz transition. By comparison with the splay angle induced by the external ac field, the authors also estimated the magnitude of the photoinduced torque. In fact, curve 1 in figure 13 gives the field derivative $\mathrm{d}A/\mathrm{d}U \approx 0.051\ \mathrm{V}^{-1}$ in the vicinity of the positive maximum of curve 2. Hence, the photoinduced absorbance $\mathrm{d}A = 2.4 \times 10^{-3}$ would correspond to the torque $\Gamma_{EL} = \Delta\varepsilon(U/d)^2/4\pi$ exerted on the director by the external voltage of $U \approx 50$ mV (U is the amplitude of the ac voltage and d is the cell thickness). Thus, for $\Delta\varepsilon = 10$ and $d = 10\ \mu$m, a photoinduced torque of the order of $\Gamma_{PH} = 0.02$ erg cm^{-3} is exerted on the director by an absorbed pump power of 10 mW (only 7% of the incident power is absorbed under the conditions considered). The qualitative model proposed by the authors for the photoinduced reorientation effects is based upon the fact that polarized light is absorbed selectively only by those molecules whose electronic oscillators are oriented parallel or at a small angle θ to the light electric vector. Since the excited dye molecules have a certain degree of orientational mobility when dissolved in low molar mass LCs then, on their orientational relaxation to the equilibrium state, they are free to choose any orientational state. In the steady-state irradiation condition the relaxed molecules will more and more populate the states with θ close to $\pi/2$ at the cost of depletion of the area near $\theta = 0$. Then, if the assumption about the freedom of the relaxed molecules to choose any orientation is fulfilled, the final orientational distribution function would be strongly anisotropic with a principal orientation of the oscillators orthogonal to the light electric vector. In a nematic LC the longitudinal axes of the dye molecules must be oriented parallel to the director. Thus, the orientational freedom of the dye molecules is limited by the existence of a uniaxial molecular field. In order to change the dye orientation and decrease the absorption, the dye oscillators should be reoriented together with the director of the LC. In this way a torque on the director is generated which, however, is not strong enough to initiate a Fredericksz-like transition from the equilibrium state. An external ac field exceeding the Fredericksz transition threshold is necessary to initialize the process. When this occurs the director can be driven by absorbing light in the direction outward from the electric light vector for positively dichroic dye and in the opposite direction for a negatively dichroic dye. In the former case (but not in the latter), the photoinduced twist distortion indeed has been observed. The different behaviour of the two guest–host systems may be accounted for by the different molecular structure of the two dyes. In fact, the molecules of the positively dichroic dye contains an azobenzene bridge which can be easily photoisomerized.

A complex reorientation phenomenology involving the superposition of photoinduced bulk and surface effects in an azo-dye-doped LC cell has recently been observed by a group of researchers including the authors of the present paper [85]. In particular we reported the first clear observation of photoinduced quasi-free sliding of the nematic director over an isotropic boundary surface endowed with very weak anchoring energy. We showed that the illumination with polarized laser light of an azo-dye doped LC cell induces both a transient dynamic sliding and a permanent reorientation of the molecular director. These two effects, that are in competition and tend to orient the director along mutually orthogonal directions, are regulated by different physical mechanisms that operate on different time scales. The scheme of the experimental setup is shown in figure 14. We used an LC cell, 20 μm thick, filled with a photosensitive mixture of 4′-n-pentyl-4-cyanobiphenyl LC (5CB) and azo-dye methyl red

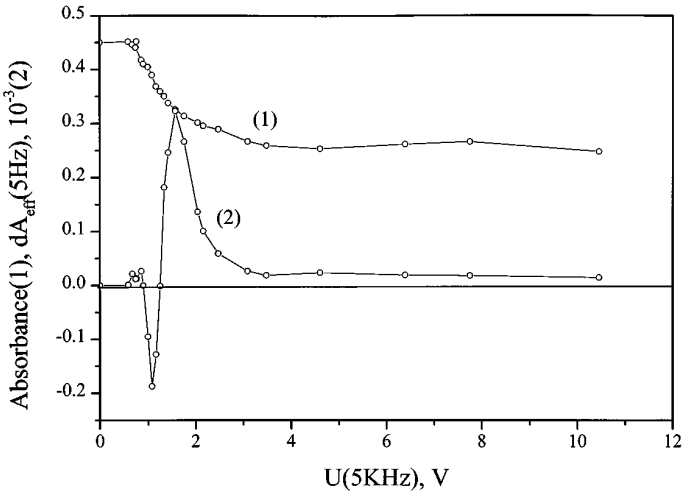

Figure 13. (1) The voltage-induced reduction of the absorbance of the probe beam (curve 1) versus the amplitude of the externally applied ac voltage. (2) The behaviour of the photo-induced absorbance for the positively dichroic azo-dye-doped sample planarly aligned along the vertical axis. The probe and pump polarization are set at $\phi = 45^\circ$ and $\beta = -45^\circ$, respectively, to the vertical axis. (After Blinovet *et al* [80].)

(MR) at weight concentration of about 1%. The inner surfaces of the two glass substrates limiting the cell were coated by different layers. The reference surface (S_r) consisted of a mechanically rubbed polyimide layer that provided strong homogeneous uniaxial anchoring. The control surface (S_c) was an untreated isotropic layer of polyvinyl-cinnamate fluoride (PVCN-F) providing a negligibly small azimuthal anchoring on the second boundary. The rubbed surface originally imposed homogeneous planar alignment of the LC molecules in the cell. The polarized pump beam from an He–Cd laser ($\lambda = 0.442$ μm; $P = 1$ mW) was focused on the cell from the side of the control surface and the director reorientation over this surface was detected by checking the polarization state of an He–Ne laser probe beam ($\lambda = 0.638$ μm) crossing the cell from the side of the reference surface. The electric field of the probe beam was set parallel to the initial director planar orientation $\boldsymbol{n}_0$, and the signal transmitted through an analyser crossed with it was detected. In this geometry [85], the measurement of the ratio of the intensity received by the analyser to the intensity of the probe beam allowed the determination of the director reorientation angle over the control surface. Figure 15 reports the dependence of the modulus of the surface director reorientation angle θ versus the time t of exposure to the exciting light, when the angle α between the incident polarization and $\boldsymbol{n}_0$ was set to 45 degrees. The initial fast rise indicates that, as consequence of the irradiation, the director $\boldsymbol{n}_c$ over the control surface rotates away from $\boldsymbol{n}_0$ towards a direction perpendicular to the incident electric vector in the plane of the isotropic surface. This behaviour can be explained in terms of a light-induced bulk torque which acts on the LC molecules of the cell caused by the reorientation of the dye molecules due to the *trans–cis* photoisomerization process occurring under irradiation in the absorption band of the dye. Because of the very small anchoring energy, the LC molecules over the isotropic surface slide out of the exciting electric vector quasi-freely and tend to align perpendicular to it. Due to the strong anchoring imposed by the rubbed surface, this reorientation results in a twisted director configuration in the bulk. This effect is not permanent as the cell spontaneously recovers its

initial planar configuration after the exciting beam is switched off.

The behaviour of $|\theta(t)|$ that follows the initial rise is a consequence of the anisotropy induced by the light on the control surface, which results in the formation of an easy-orientation axis parallel to the exciting field [78, 79]. The mechanism responsible for this process seems to be the adsorption on the isotropic surface of the MR molecules which undergo phototransformation. As the exposure time increases, the director rotates over the control surface towards the easy axis and finally reorients parallel to it. The consequent twisted director configuration which is set up in the cell is extremely stable: no change in the irradiated area was found after several months. This effect has been exploited to record high-resolution intensity [82] and polarization [83] holographic gratings in liquid crystal. The interpretation of the experimental results in terms of a competition between sliding and capturing was confirmed by measurements in which the anchoring energy of the easy axis was varied by pre-illumination of the sample before irradiation (see the inset of figure 15).

A simple phenomenological model has been proposed which accounts for the above experimental observations. According to this, two different mechanisms contribute to the director reorientation over the control surface: the bulk torque due to the photoinduced reorientation of the MR molecules, which favours director alignment perpendicular to the exciting polarization, and the surface torque associated with the adsorption of the phototranformed MR molecules, which favours alignment parallel to the incident polarization. The competition between these effects controls the reorientation process. On the other hand, the direct optical torque of the light field on the LC molecules can be neglected because of the small intensity used in the experiments. The total free energy of the system was then written as

$$F = \frac{1}{2}K\int[(\boldsymbol{\nabla}\cdot\boldsymbol{n})^2 + (\boldsymbol{\nabla}\times\boldsymbol{n})^2]\,\mathrm{d}V + \chi\int(\boldsymbol{n}\cdot\boldsymbol{e})^2\,\mathrm{d}V - w\int c_s(\beta)(\boldsymbol{n}_c\cdot\boldsymbol{l})^2\,\mathrm{d}\beta\,\mathrm{d}S \quad (86)$$

where the three terms represent the elastic, the bulk-reorientation and the surface-reorientation contribution, respectively, K is the elastic constant of the LC in the one constant approximation, $\boldsymbol{n}$ is the director in the bulk, $\boldsymbol{e}$ is the unit vector of the incident polarization, χ ($\chi > 0$) is a quantity measuring the strength of interaction between MR and LC molecules, $\boldsymbol{l} = (\cos\beta, \sin\beta, 0)$ is the unit vector giving the local easy-axis direction for the surface director reorientation due to MR adsorption, $c_s(\beta)$ is the anisotropic angular distribution of the surface concentration of adsorbed MR molecules, and w ($w > 0$) is a quantity characterizing the strength of interaction between LC and adsorbed MR molecules. The assumption of a reliable model for the surface molecular adsorption [79, 85] allowed us to write the rate of adsoption $P(t)$ as

$$P(t) = c_0(a' + b'c_{s0}(t))E^2\nu k(\boldsymbol{l}_1\cdot\boldsymbol{e})^2 \quad (87)$$

where c_0 is the volume concentration of MR, a' and b' are proportionality constants, $c_{s0}(t) = \int c_s(\beta, t)\,\mathrm{d}\beta$ is the total concentration of adsorbed MR molecules, $\boldsymbol{l}_1 = (\sin\varphi\cos\beta, \sin\varphi\sin\beta, \cos\varphi)$ is the unit vector giving the orientation of MR molecules in the interfacial region near the control surface, ν is the quantum efficiency of the adsorption process and k is the absorption coefficient along the dye molecular axis. Considering that the probability for the adsorbed dye molecules to have orientation $\boldsymbol{l}$ on the control surface is proportional to $\int P(t, \varphi, \beta)\sin\varphi\,\mathrm{d}\varphi$ and after integrating over φ, the kinetic equations for c_s and c_{s0} became

$$\begin{aligned}\frac{\mathrm{d}c_s(\beta, t)}{\mathrm{d}t} &= c_0(a + bc_{s0}(t))E^2\nu k(\boldsymbol{l}\cdot\boldsymbol{e})^2\\ \frac{\mathrm{d}c_{s0}(t)}{\mathrm{d}t} &= c_0(a + bc_{s0}(t))\pi E^2\nu k\end{aligned} \quad (88)$$

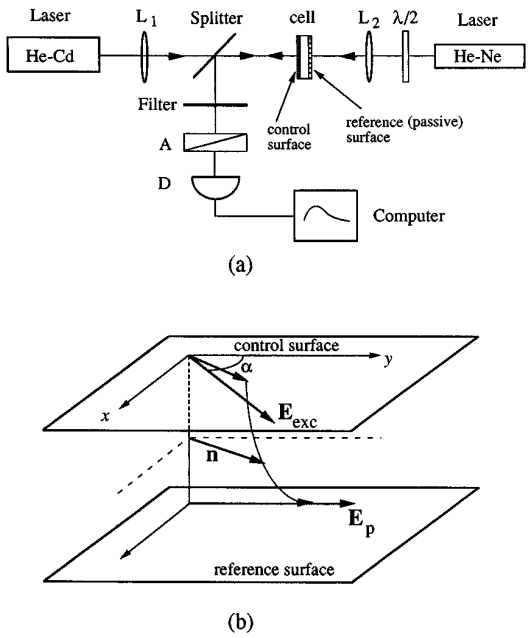

Figure 14. (a) Experimental setup: L_1 and L_2, lenses; BS, beam splitter; $\lambda/2$, half-wave plate; LC, liquid crystal cell; F, filter; A, analyser; P, photodetector; C, computer. (b) Detail of the LC cell. $E_{\rm exe}$ is the electric field of the exciting beam, $E_{\rm P}$ is the electric filed of the probe beam.

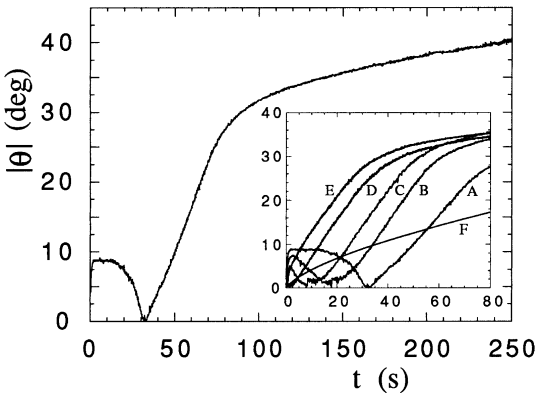

Figure 15. Modulus of the surface director reorientation angle θ versus the exposure time t when $\alpha = 45^\circ$. A change of sign occurs in θ when the curve crosses the time axis. The inset shows a set of $|\theta|$–t curves measured after pre-illuminating the sample for different times t_0 before irradiation: (A) $t_0 = 0$ s; (B) $t_0 = 10$ s; (C) $t_0 = 20$ s; (D) $t_0 = 50$ s; (E) $t_0 = 120$; (F) $t_0 = 360$ s. Pre-illumination was achieved by subjecting the sample to an incident lightfield (from an He–Cd laser) parallel to $\boldsymbol{n}_0$; this induces an easy axis parallel to $\boldsymbol{n}_0$ whose anchoring energy increases with t_0. (After Francescangeli *et al* [85].)

with $a = 4a'/3$, $b = 4b'/3$. Solution of the coupled equations (88) with the initial condition $c_s(\beta, 0) = 0$ gave $c_s(\beta, t) = a(b\pi)^{-1}[\exp(t/\tau) - 1]\cos^2(\alpha - \beta)$ where $\tau = (c_0 b\pi \nu E^2 k)^{-1}$. In the presence of pre-illumination of the sample for a time interval t_0 with light polarized parallel to the x axis ($\alpha = 0$), and of subsequent irradiation with light polarized at an angle α, the angular distribution of adsorbed dye molecules at time t ($t > t_0$) became

$$c_s(\beta, \alpha, t)_{t \geqslant t_0} = a(b\pi)^{-1}[(\exp(t_0/\tau) - 1)\cos^2\beta + (\exp(t/\tau) - \exp(t_0/\tau))\cos^2(\alpha - \beta)]. \tag{89}$$

The corresponding surface free energy was then

$$F_S = WS[(\exp(t_0/\tau) - 1)\cos^2\theta + (\exp(t/\tau) - \exp(t_0/\tau))\cos^2(\alpha - \theta)] \tag{90}$$

where $W = wa/(2b)$ and S is the area of the control surface. The time evolution of the reorientation process was found by standard minimization of the total free energy, linearization of the Euler–Lagrange equation and solution with the appropriate boundary conditions. In this way we obtained for the surface reorientation angle θ

$$\theta(t, t_0) = -\frac{\chi_0 c_v L^2}{K}\frac{1}{1 - 2\xi_1(t_0)} - \frac{\xi_2(t, t_0)}{1 - 2\xi_1(t_0)} \tag{91}$$

where $\xi_1(t_0) = 2WLK^{-1}(\exp(t_0/\tau) - 1)$ and $\xi_2(t, t_0) = 2WLK^{-1}(\exp(t/\tau) - \exp(t_0/\tau))$ are the anchoring parameters and $\chi = \chi_0 c_v$. Equation (91) provides a satisfactory reproduction of the experimental results. The first term describes reorientation perpendicular to the light polarization ($\theta < 0$) while the second term describes reorientation towards the exciting polarization ($\theta > 0$); $\theta = 0$ corresponds to the mutual compensation of the bulk and surface torques.

The optical reorientation of nematic LCs in the presence of photoisomerization has been recently investigated by Jánossy and Szabados [89] with special attention to the dependence of the induced torque on the angle β between the wavevector of the light beam and the nematic director. The paper was motivated by previous experimental observations of other authors [90] who reported a series of results on azo-dye-doped LCs which seemed to contradict the existing models. In particular Barnik *et al* found that, in their system, the absorption-induced torque changed sign as the angle β was varied; namely, it was negative for small angles and became positive above a critical angle. In the general Jánossy picture of the photoinduced reorientation in dye-doped LCs, the presence of the absorbing dye reflects into an enhancement of the classical optical torque (see equation (75)). This enhancement of the torque has been explained by several authors as the effect of an angularly selective resonant excitation of anisotropic dye molecules, whose probability is proportional to the cosine squared of the angle between the director and the exciting electric field. Then, the angular distribution of excited molecules is tilted in the direction of the field, while that of molecules remaining in the ground state is tilted perpendicularly to the field. If the attractive potential between dye and LC molecules is stronger for excited than for unexcited dye molecules, the director is submitted to an attractive torque toward the light electric field. In the opposite case, the dye-induced resonant torque repels the director from the field. Indeed, rotations in both directions have been observed as previously reported. In [89] a model is proposed where the *trans* and *cis* forms of azo-compounds are regarded as two separate dye dopants that contribute with different strengths or even sign to the overall optical torque. The anomalous angular dependence of optical reorientation reported in [90] is then explained by considering the photoinduced *trans–cis* equilibrium as discussed in the following.

In liquid crystals, at the low light intensities used for isomerization, the orientational distributions of both the *trans* and *cis* isomers basically correspond to a thermodynamic

equilibrium, even during the isomerization process. In fact, the characteristic times for photoisomerization are typically several orders of magnitude larger that the typical rotational diffusion times for molecules in the nematic phase. These equilibrium distributions are inherently anisotropic and the symmetry axis coincides with the direction of the nematic director. However, the extent of orientational order is different for the two isomers. In particular the *trans* molecules, which have an elongated shape, should be more effectively oriented along the LC host molecules than the V-shaped *cis* isomers. The former molecules should therefore give a significantly higher contribution to the dichroism of the liquid crystal than the latter ones. By light irradiation it is possible to change the *cis* concentration and, as a consequence, the magnitude of the anisotropy of the guest–host system. This result has been experimentally verified by using a pump–probe technique [91]. For low dye concentrations, as it is in most applications, the orientational distribution functions of the *trans* and *cis* isomers are independent and are determined only by the guest–host interaction between the LC molecules and the isomer. In thermal equilibrium the molecules are in the *trans* form. Light irradiation converts a fraction of the molecules to the *cis* form. When the pump beam is applied to the LC-dye mixture, the concentration of the *cis* molecules N_C obeys the rate equation

$$\frac{\mathrm{d}N_C}{\mathrm{d}t} = (N_T\sigma_T^i\Phi_{TC} - N_C\sigma_C^i\Phi_{CT})I/h\nu - N_C/\tau \tag{92}$$

where the first term on the right-hand side describes the light-induced transitions whereas the second term represents the thermal-induced *cis–trans* transitions (characterized by relaxation time τ). In equation (92) Φ_{TC} and Φ_{CT} are the quantum efficiencies of the *trans–cis* and *cis–trans* transitions, respectively, N_T is the concentrations of the *trans* isomers, I the intensity of the incident light, σ_T^i and σ_C^i are the absorption cross sections of a photon with energy $h\nu$ for a *trans* and a *cis* isomer, respectively (averaged over the orientational distribution function of the relevant isomer). The index i refers to the polarization direction of the pump beam and can correspond to the extraordinary (e) or to the ordinary (o) ray. For the extraordinary ray, the averaged cross sections depend on the angle between the light wavevector and the director. If we introduce the *trans* and *cis* absorption coefficients defined as

$$\alpha_T^i = N\sigma_T^i \qquad \alpha_C^i = N\sigma_C^i \tag{93}$$

where $N = N_T + N_C$ is the total number of dye molecules per unit volume, then the attenuation α^p of a probe beam polarized along the p direction when crossing a sample containing a fraction $X = N_C/N$ of *cis* isomers, is given by

$$\alpha^p = (1 - X)\alpha_T^p + X\alpha_C^p. \tag{94}$$

In steady-state conditions $\mathrm{d}N_C/\mathrm{d}t = 0$ and, from equation (92), the equilibrium value of the *cis* fraction, $X = X_{eq}^i$, is found to be

$$X_{eq}^i = \frac{X_S^i}{1 + I_S^i/I} \tag{95}$$

where the intensity parameter I_S^i is given by

$$I_S^i = \frac{\sigma_C^i\Phi_{CT} + \sigma_T^i\Phi_{TC}}{\tau h\nu} \tag{96}$$

and the quantity

$$X_S^i = \frac{\sigma_T^i A}{\sigma_C^i + A\sigma_T^i} = \frac{\alpha_T^i A}{\alpha_C^i + A\alpha_T^i} \qquad \text{with } A = \Phi_{TC}/\Phi_{CT} \tag{97}$$

is the saturation value of the *cis* fraction at intensities much higher than I_S. Using a pump–probe technique, the absorption coefficients of the *trans* and *cis* isomers can be evaluated

separately and the dye order parameters of both forms can be determined too. If we consider a probe beam polarized in the r direction and propagating in the same direction as the pump beam, the probe absorption coefficient belonging to the steady-state conditions is

$$\alpha_{ir} = (1 - X^i_{eq})\alpha^r_T + X^i_{eq}\alpha^r_C. \tag{98}$$

The parameters involved in the model can then be determined by measuring α_{im} as a function of the pump intensity corresponding to the four possible combinations of the pump and probe polarizations ($i = e, o$ and $r = e, o$). In this way one obtains [91]

$$A = \frac{\alpha^e_T - \alpha_{ee}}{\alpha_{ee} - \alpha_{oe}}\left(\frac{\alpha_{oe}}{\alpha^e_T}\frac{\alpha_{oo}}{\alpha^o_T}\right) = \frac{\alpha^o_T - \alpha_{oo}}{\alpha_{oo} - \alpha_{eo}}\left(\frac{\alpha_{eo}}{\alpha^o_T} - \frac{\alpha_{ee}}{\alpha^e_T}\right) \tag{99}$$

$$\alpha^e_C = \frac{\alpha_{ee}\alpha^e_T A}{\alpha^e_T(A+1) - \alpha_{ee}} \qquad \alpha^o_C = \frac{\alpha_{oo}\alpha^o_T A}{\alpha^o_T(A+1) - \alpha_{oo}}. \tag{100}$$

Once A, α^e_T, α^o_T, α^e_C, α^o_C are determined the principal values of the absorption coefficients $\alpha_\parallel$ and $\alpha_\perp$ (polarization direction parallel and perpendicular to the director) can be determined using the laws of standard optics [3]. The experimental results obtained with this technique indicate that the *trans* form possesses a much higher dichroism than the *cis* one due to the different degree of orientational order of the dye molecules. Figure 16 shows an example of the wavelength dependence of both the *trans* and *cis* order parameters of the azo-dye Disperse Orange 3 (DO3) when mixed (0.5 wt%) with the nematic E63 in an LC cell. The data show that the *cis* molecules still exhibit a non-zero orientational order. On a molecular level, the dye order parameter basically reflects the degree of order of the transition dipole moment of the dye molecules. The large decrease of the dye order parameter upon isomerization is a result of several contributions. First, the disorder of the long axis of the molecule (i.e. the axis corresponding to the smallest moment of inertia) is more important for the *cis* form than for the *trans* one due to the difference in shape of the two conformers. Second, the angle between the transition dipole moment and the long axis may be different for the two isomers. Third, the *cis* molecules may not rotate freely about their long axis.

These results clearly point out that in nematics the steady-state concentration of *cis* isomers can be controlled, at fixed wavelength, also through the polarization direction of the pump beam. An inspection of equations (95)–(100) shows that the saturation *cis* concentrations for $i = o$ and $i = e$ are different from zero whenever the dye order parameters of the *trans* and *cis* forms are not equal. This fact indicated that the polarization dependence of the *trans–cis* equilibrium is connected with the difference of the dye-order parameters of the two isomers.

The above equations for the *trans–cis* equilibrium can be conveniently expressed in terms of the probabilities $p_C = \sigma^i_C I/h\nu$ and $p_T = \sigma^i_T I/h\nu$ that a *cis* and *trans* molecule, respectively, is excited within a unit time. In particular, equation (95) for the equilibrium *cis* fraction can be rewritten (omitting the polarization index i and writing simply X for X_{eq}) as

$$X = \frac{X_S}{1 + \tau_0/\tau} \tag{101}$$

where

$$X_S = \frac{p_T\Phi_{TC}}{p_T\Phi_{TC} + p_C\Phi_{CT}} \qquad 1/\tau_0 = p_T\Phi_{TC} + p_C\Phi_{CT} \tag{102}$$

and τ_0 is the characteristic time for the formation of the steady-state *cis* concentration. This characteristic time decreases as the light intensity is increased; in typical reorientation experiments the light intensity is high enough to saturate the number of *cis* isomers. As shown by equations (101) and (102), a polarization dependence of the excitation probabilities is reflected in a polarization dependence of the *trans–cis* equilibrium. To quantify this effect,

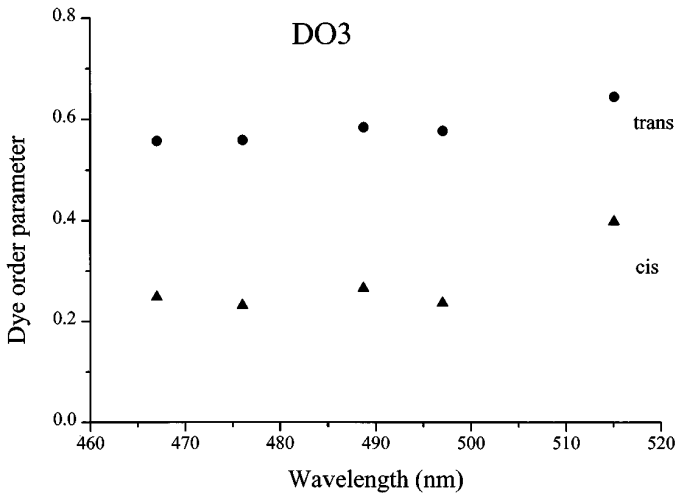

Figure 16. Wavelength dependence of the *trans* and *cis* order parameters of the azo-dye Disperse Orange 3 (DO3) when mixed (0.5 wt%) with the nematic E63 in an LC cell. (After Jánossy and Szabados [91].)

let us first consider the dissipated energy per unit time and volume, W_D, assuming a single dye dopant in the LC mixture. In terms of microscopic quantities it can be written as $W_D = h\nu Np$ (p is the excitation probability per unit time) whereas macroscopically it is given by $W_D = \varepsilon_0 2\pi\nu E^2 \boldsymbol{e}\underline{\varepsilon}''\boldsymbol{e}$, where $\underline{\varepsilon}''$ is the imaginary part of the dielectric tensor, E is the effective electric field and $\boldsymbol{e}$ is a unit vector along the electric field. The components of $\underline{\varepsilon}''$ in the nematic LC can be written as $\varepsilon''_{ij} = \varepsilon''_\perp \delta_{ij} + (\varepsilon''_\parallel - \varepsilon''_\perp) n_i n_j$ where $\boldsymbol{n}$ is the director, therefore

$$W_D = \varepsilon_0 2\pi\nu[\varepsilon''_\perp + (\varepsilon''_\parallel - \varepsilon''_\perp)\cos^2\Psi]E^2 \tag{103}$$

where Ψ is the angle between $\boldsymbol{n}$ and $\boldsymbol{e}$. Comparing equation (103) with the microscopic expression for W_D one finds

$$p = [f_\perp + (f_\parallel - f_\perp)\cos^2\Psi]E^2 \qquad \text{with } f_\perp = 2\pi\varepsilon''_\perp/Nh \text{ and } f_\parallel = 2\pi\varepsilon''_\parallel/Nh. \tag{104}$$

In the limit of low concentration of azo-dye and low light intensity the two isomers can be regarded as two independent dopants with the orientational distributions corresponding to a thermal equilibrium. Equation (104) then holds separately for both isomers; i.e.

$$\begin{aligned} p_C &= [c_\perp + (c_\parallel - c_\perp)\cos^2\Psi]E^2 \\ p_T &= [t_\perp + (t_\parallel - t_\perp)\cos^2\Psi]E^2 \end{aligned} \tag{105}$$

where the coefficients c and t depend on the molecular parameters and the orientational order of the isomers, but are independent of the dye concentration and X. Inserting equations (105) into equation (102) one finds for an ordinarily polarized beam

$$X_S = X_{ord}\frac{1 + g\cos^2\Psi}{1 + h\cos^2\Psi} \tag{106}$$

with

$$X_{ord} = \frac{At_\perp}{At_\perp + c_\perp} \qquad g = \frac{t_\parallel - t_\perp}{t_\perp} \qquad h = \frac{A(t_\parallel - t_\perp) + c_\parallel - c_\perp}{At_\parallel + c_\perp} \tag{107}$$

and $A = \Phi_{TC}/\Phi_{CT}$. The parameter X_{ord} in equations (106) and (107) gives the saturated *cis* concentration for an ordinarily polarized beam and represents a quantity independent of the light propagation direction. The angular dependence (i.e. the dependence on Ψ) of X predicted by equation (106) has been experimentally verified by pump–probe experiments in dye-doped nematic mixtures [90]. The angular dependence of the optical torque was then obtained [90] by writing the additional absorption-induced torque in terms of an enhancement factor η as previously discussed, i.e. $\boldsymbol{\Gamma}_{DYE} = \eta\boldsymbol{\Gamma}_{OPT}$. The fundamental difference is that in the presence of azo-dyes, we can regard the two *trans* and *cis* isomers as separate dyes which give independent contributions to the absorption-induced torque. Thus, the enhancement factor can be written as

$$\eta = X\eta_C + (1 - X)\eta_T = \eta_T + (\eta_C - \eta_T)X \tag{108}$$

where η_C and η_T characterize the strength of the absorption-induced torque for the *cis* and *trans* isomers, respectively, and have no angular dependence. If the intensity of the incident light is sufficient to saturate the *cis* concentration, then $X = X_S$ and the angular dependence of η is expressed by equation (109)

$$\eta = \eta_T + (\eta_C - \eta_T)X_S \tag{109}$$

where X_S is given by equation (106). The experimental determination of the enhancement factor has been performed by comparing optical reorientation in a doped and undoped sample under the same geometrical conditions [89]. As an example figure 17 reports the η values as a function of the angle of incidence of the pump beam for two different dyes, one of which (R4) is photoisomerizable. The results clearly show the striking qualitative difference in the behaviour of isomerizable and non-isomerizable dyes. The experiments also allow the determination of η as a function of X_S. In particular, the linear behaviour predicted by equation (109) has been shown to be satisfied for the azo-dye-doped mixture, with a positive value for η_C and a negative value for η_T. According to this model, the angular dependence of the enhancement factor η is a consequence of the variation of the equilibrium of the *cis* fraction with the light propagation direction. When the pump beam is extraordinarily polarized, as it was in these experiments, its propagation direction determined X_S and thus η. The presence of a superposed ordinarily polarized component in the pump beam modifies the *trans–cis* equilibrium. Thus, according to this model, although an ordinarily component in itself does not induce director reorientation, it should influence the optical torque exerted by the extraordinary ray by changing the value of X_S and therefore the enhancement factor. If the electric field $\boldsymbol{E}$ of the incident beam is $\boldsymbol{E} = E_e\boldsymbol{e}_e + E_o\boldsymbol{e}_o$, where $\boldsymbol{e}_e$ and $\boldsymbol{e}_o$ are the polarization vectors for the extraordinary (e) and ordinary (o) ray, respectively, one finds that the dissipated energy W_D is an independent superposition of the dissipations of the e and o components, and the same holds for the excitation probabilities. Thus one finds [90]

$$X_S = X_{ord}\frac{1 + g\cos^2\Psi\cos^2\Theta}{1 + h\cos^2\Psi\cos^2\Theta} \tag{110}$$

with $\tan\Theta = E_o/E_e$, and

$$\eta = \eta_T + (\eta_C - \eta_T)X_{ord}\frac{1 + g\cos^2\Psi\cos^2\Theta}{1 + h\cos^2\Psi\cos^2\Theta}. \tag{111}$$

The experimental findings presented in [90] show that the *trans* and *cis* enhancement factors of azo-dye-doped nematic LCs are comparable with the values measured for the most effective anthraquinone dye at similar concentrations. In addition, it was found that the optical torques, generated by *trans* and *cis* isomers, are of opposite signs, namely, negative for the former and positive for the latter isomer. In the presence of photoisomerization the resultant

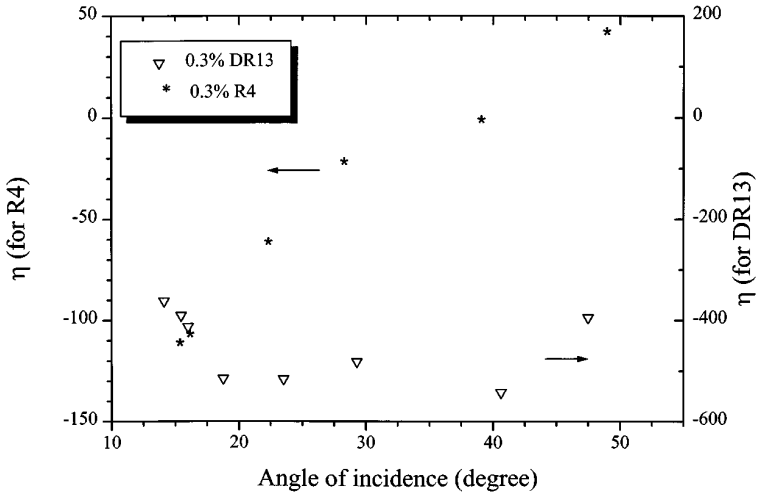

Figure 17. The enhancement factor η as a function of the incidence angle for the dyes 4′-dimethylaminophenyl-[1,4-phenylenebis(azo)]-3-chloro-4-heptyloxy benzene (R4) and 2-[4-(2-choloro-4-nitrophenylazo)-N-ethyl-phenylamino]ethanol (DR13). (After Jánossy and Szabados [89].)

enhancement is significantly reduced because the contributions from the two isomers tend to cancel each other.

Finally, very recent experimental results [92] of the director reorientation in a homeotropic nematic LC cell ($\boldsymbol{n}$ perpendicular to the cell substrates) doped with the bisazobenzene dichroic dye D2 showed that photoexcitation of the dye creates a resonant torque that is not coplanar with the traditional dielectric torque. These results confirmed previous observations made by Khoo and coworkers [93] on the dynamic grating formation in a planar LC cell ($\boldsymbol{n}$ parallel to the cell substrate) doped with the same dye D2. In particular, the polarization-dependence study of the laser-induced director reorientation in ref. [93] showed that the excited dye molecules caused reorientation of the LC director axis in both directions orthogonal to the initial molecular alignment (in the field of two interfering laser beams). Similar excitation phenomena were observed by Saad *et al* [92] in a D2-doped homeotropic nematic LC cell. The dynamics of the buildup of the light-induced grating have shown three principal regimes, one of which was interpreted as a three dimensional (3D) rotation of the director and was attributed to the photoisomerization of D2 dye molecules. These authors also reported a detailed investigation of the excitation along with the steady-state and the non-monotonic relaxation dynamics. The photo-induced torque was found to initiate a reorientation that was significantly out of the symmetry plane during the transient regime of excitation and relaxation. In addition, they showed that the reorientation paths that the director follows in the excitation and the relaxation processes are different. A schematic representation of the interaction geometry is shown in figure 18(a). The excitation and relaxation dynamics of nematic LC birefringence were detected by pure horizontal and vertical probe polarizations. The measured non-monotonic transmission behaviour during excitation was explained as due to a particular out-of-plane trajectory of the director with the in-plane symmetry of the initial director and of the excited field (figure 18(b)). A non-monotonic behaviour of relaxation was also observed which, together with the exact symmetry of the variations of both the vertical and horizontal polarization components, proved

an out-of-plane trajectory of the director in this case too. Furthermore, the opposite signs of the excitation and relaxation signals showed that the trajectories of the director are opposite with respect to the horizontal plane, but not exactly symmetric, since in the presence of the exciting beam the steady state of the director is not exactly in the horizontal plane. In other terms, during the transient excitation the birefringence extraordinary axis rotates in the direction of the chosen probe polarization whereas during the transient relaxation the rotation occurs in the opposite direction. In addition, for both excitation and relaxation, the out-of-plane component of the director is significant only during the transient regime. The origin of the observed 3D transient rotation is not clear as it corresponds to a break in the apparent symmetry of the excitation and of the nematic LC together. The origin of the observed phenomena is probably in the complex coupling of photoisomerizing dye with nematic host.

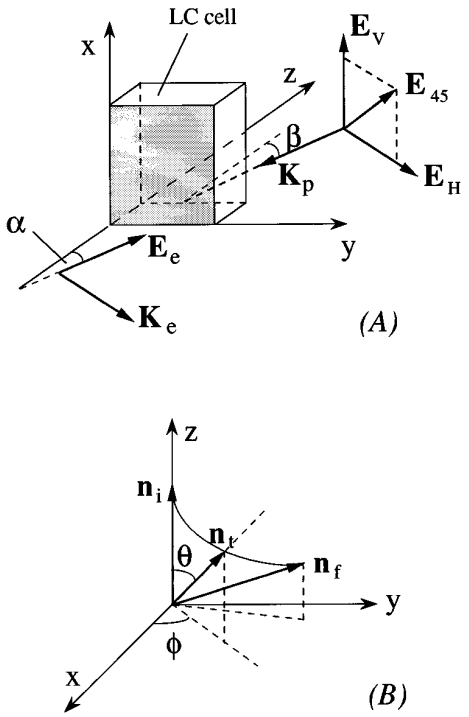

Figure 18. (a) Schematic representation of the interaction geometry. $\boldsymbol{E}_e$ and $\boldsymbol{K}_e$ are the electric field and the wavevector, respectively, of the linearly polarized exciting beam from a c.w. Ar ion laser. Both vectors lie in the yz plane. $\boldsymbol{E}_V$, $\boldsymbol{E}_H$ and $\boldsymbol{E}_{45}$ are the electric vectors corresponding to three different polarizations of the probe beam: $\boldsymbol{E}_H$ is in the horizontal yz plane, $\boldsymbol{E}_V$ is parallel to the vertical x direction whereas $\boldsymbol{E}_{45}$ is in the plane defined by $\boldsymbol{E}_V$ and $\boldsymbol{E}_H$, at 45° to the x axis. $\boldsymbol{K}_p$ is the wavevector of the probe beam, which lies in the yz plane. α and β are the excitation and probe beam incidence angles. The detection is made through a horizontal analyser or a Wollaston prism splitting the probe into its vertical and horizontal components. (b) Geometry of interaction: $\boldsymbol{n}_i$ is the starting director orientation of the unperturbed cell (parallel to the z axis); $\boldsymbol{n}_t$ is the 3D transient director orientation defined by the polar and azimuthal angles θ and ϕ, respectively; $\boldsymbol{n}_f$ is the final director orientation under steady-state irradiation ($\boldsymbol{n}_f$ is almost in the horizontal yz plane). The curved solid line represents the trajectory of the director when the excitation beam is switched on.

4. Photorefractivity

4.1. General aspects of the effect

The photorefractive effect (PR) consists in the spatial modulation of the refractive index due to the light-induced redistribution of charge carriers in an optically nonlinear material. Photorefractivity was first observed in 1966 in inorganic ferroelectric crystals [94] and it was soon realized that it could be used for image storage and a variety of optical signal processing applications [95]. The PR effect arises when charge carriers, which are photogenerated by a spatially modulated light intensity, separate by unidirectional migration over macroscopic distances within the material and finally become trapped. This creates a space-charge field which modulates the index of refraction through the electrooptic effect [96]. Photorefractivity is quite different from most of the other NLO effects in that it cannot be described by a nonlinear susceptibility $\chi^{(n)}$ for any value of n. In fact, under a wide range of conditions, the steady-state change in refractive index is independent of the intensity of the light that induces the change.

The basic processes involved in the photorefractive effect are illustrated schematically in figure 19. A pair of coherent laser beams that are crossed in a photorefractive material produce an interference pattern (figure 19(a)) that photogenerates charge carriers in the illuminated regions. These charges can diffuse through the crystal or can drift in response to a static electric field to produce a nonuniform space-charge distribution (figure 19(b)). The resulting space-charge field (figure 19(c)) modulates the refractive index via the linear electrooptic effect (Pockels effect), thus producing a refractive index grating (figure 19(d)) which can diffract a light beam. The magnitude of the index modulation Δn is related to the magnitude of the space-charge field $\boldsymbol{E}_{sc}$ by equation (112)

$$\Delta n = -\tfrac{1}{2}n^3 r_e E_{sc} \tag{112}$$

where n is the optical index of refraction and r_e is the effective electrooptic coefficient for the geometry under consideration. Many other mechanisms exist which can modify the index of refraction of a material in response to an optical beam, such as photochromism, thermochromism, thermorefraction, generation of excited states and so forth. However, all of these local mechanisms lack the nonlocal property of the PR effect arising from the physical motion of charges in the material. This charge transport gives rise to a spatial shift between the incident light intensity pattern and the refractive index modulation. An important consequence of this phase shift is the energy transfer that occurs between the two light beams interfering in the PR medium, an effect which is known as asymmetric two-beam coupling (TBC); the measurement of this energy transfer is the best diagnostic method for the occurrence of the photorefractive effect in thick gratings. Photoionizable charge generation, efficient charge transport over macroscopic distances and diffusion anisotropy are the primary requirements for producing the space-charge field necessary for photorefractivity. Trapping sizes are also desirable for long-lived storage of the space-charge field.

A remarkable advance in the field of photorefractivity came in 1991 with the discovery of the photorefractive effect in organic polymers [97]. Optical nonlinearity in polymers is provided by adding to a photoconductive polymeric matrix a large concentration ($\approx$30 wt%) of relatively small NLO chromophores, i.e. particular molecules which can be reoriented by an external applied field. These are in general asymmetrically substituted molecules with an electron-donating moiety and an electron-accepting moiety separated by a conjugated structure. To obtain a macroscopic electrooptic effect the originally randomly oriented chromophores must be aligned by a dc electric field. This field also assists the charge photogeneration by reducing the recombination probability and provides the force for drifting the charge carriers. Charge transport is usually provided by including in the material special molecules termed

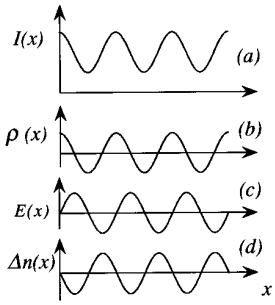

Figure 19. Origin of the photorefractive effect. (a) A photorefractive medium illuminated by two interfering beams that produce a spatially modulated intensity distribution $I(x)$. (b) Free charge carriers, electrons in this case, are generated through photoionization and can diffuse from regions of maximum optical intensity to regions of minimum intensity thus creating a spatially modulated charge distribution $\rho(x)$. (c) Since the Poisson equation relates the spatial gradient of the electric field to the charge distribution $\rho(x)$, the resulting internal electric field $E(x)$ is shifted by 90 degrees from the light intensity pattern. (d) A refractive index variation is produced in the electrooptically active material through the linear electrooptic effect.

charged transport agents so that charge carriers can hop from one charge-transporting moiety to another [98]. At present photorefractive polymers have higher net photorefractive gain than do their inorganic single crystal counterparts. Such high performances have been achieved both through optimization of the charge generation, charge transport and electrooptical characteristics of the doped polymers and through a continuous reduction of the glass transition temperature T_g of the polymers. This latter effect assumes a particular relevance since it permits orientational alignment of the birefringent NLO chromophores by a space-charge field within the viscous polymer. This nonlinear electrooptic effect, which is called the *orientational* electrooptic effect, produces an additional large contribution to the total change in the index of refraction which can be greater than that of the traditional linear electrooptic effect [99, 100]. This enhancement relies on the ability of NLO chromophores to be aligned not only by the external applied electric field, but also *in situ* by the sinusoidally modulated space-charge field during grating formation [101]. The resulting spatially periodic poling of the sample leads to a modulation of the birefringence and of the electrooptic response. The combination of these effects contributes favourably to the diffraction efficiency. Figure 20 describes this effect schematically. The interfering light beams are assumed to create a sinusoidally modulated space-charge field $E_{sc}(x)$ by the usual mechanisms of drift or diffusion (for simplicity the two writing beams are assumed to enter the sample from the right and left sides of the figure). An external electric field E_0 is applied that adds to this field to produce a total field $E(x)$. As the NLO chromophores have orientational mobility due to the low T_g, a spatially periodic orientational pattern is produced as the electric field reorients the molecules by virtue of their ground-state dipole moment. If $\boldsymbol{E}_0$ and $\boldsymbol{E}_{sc}$ have the same direction, as in figure 20, only the magnitude of the average local dipole moment will be periodic. In the more general case of oblique incidence, where there is a component of $\boldsymbol{E}_0$ orthogonal to $\boldsymbol{E}_{sc}$, the direction of the average local dipole moment will be periodic as well [99]. The effect of the periodic orientation is to produce a modulated birefringence and a modulated electrooptic coefficient. In this situation the NLO response of the material is quadratic in the total electric field, hence the orientational enhancement effect may be regarded formally as a third order NLO effect ($\chi^{(3)}$ process). This quadratic electrooptic effect should be operative for any photorefractive polymer in which the NLO chromophores possess the ability to reorient

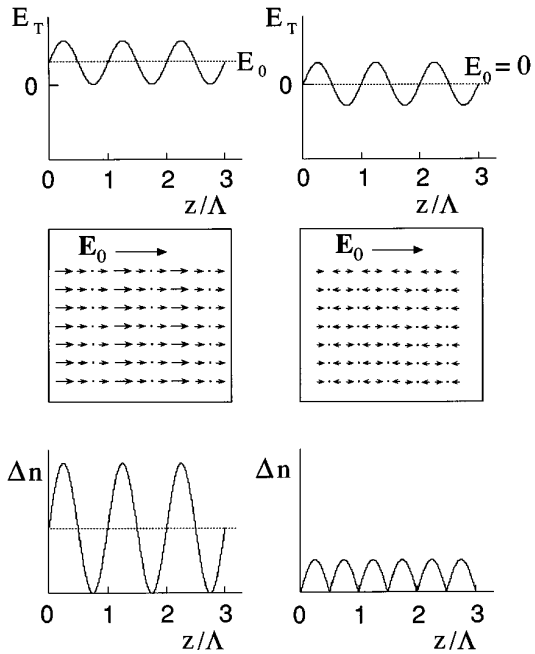

Figure 20. Simplified model of the periodic poling responsible for the orientational enhancement effect. For the sake of simplicity, the writing beams are supposed to propagate in opposite directions along the z axis and to enter the sample from either side of the figure (symmetrically). In this way, the background field E_0 and the space charge field are both directed along z. The figure at the top shows the magnitude of the total field for the case $E_0 \neq 0$ (left) and $E_0 = 0$ (right). The resulting average alignment of the chromophores is shown in the centre whereas the bottom panels report the resulting refractive index grating. If the grating is written in the oblique geometry, an additional component of dc field appears perpendicular to z, which results in a modulated direction as well as magnitude of the periodic poling field. (After Moerner and Silence [101].)

appreciably in response to the local electric field and leads to refractive index variations Δn of the order of 10^{-2}–10^{-3}, i.e. three orders of magnitude higher than in traditional inorganic photorefractive crystals. Since this orientation enhancement depends on the ability of the NLO chromophores to orient dynamically during the grating formation, the speed of the effect is limited by the rotational mobility of the chromophores in the polymeric matrix. The theory of the orientational enhancement of the refractive effect [99] predicts an enhanced diffraction efficiency, a change in the polarization anisotropy and the presence of gratings with wavevectors that are multiple of the wavevector $\boldsymbol{q}$ of the intensity pattern, even with a purely sinusoidal space-charge field. In the framework of this model, the sinusoidal space-charge grating produces a sinusoidal birefringence and a sinusoidal modulation of the electrooptic coefficient, both of which contribute an orientational enhancement to the scattered optical field.

4.2. Photorefractivity in conventional nematic LCs

On the basis of the results and considerations of the previous paragraph, nematic liquid crystals appear to be extremely promising materials for photorefractivity. This is because nematic LCs consist entirely of long rod-shaped molecules that produce greater bulk birefringence than does a polymer that is merely doped with a birefringent chromophore. Also, LCs have directional

order despite their low viscosity, which allows for greater orientational displacement for a given space-charge field. Finally, differently from photorefractive polymeric materials that require large electric field to pole the material and to obtain a bulk electrooptic effect, LCs require only a weak electric field to induce directional charge transport and to enhance the quadratic electrooptic effect. Indeed there are few materials that can be compared to LCs for maximizing the quadratic electrooptic effect. The low electric fields required for reorienting liquid crystals, combined with their high birefringence, result in the observation of photorefractivity with very low optical intensities ($\approx$100 mW cm^{-2}) and low applied fields ($\approx$100–400 V cm^{-1}). For all these reasons, photorefractive liquid crystals actually represent an emerging class of new materials [102, 103].

The first observation of photorefractivity in liquid crystals was reported by Rudenko and Sukhov in 1994 [104–106], who attributed the effect to a space-charge field arising from the photoinduced conductivity anisotropy. They used the nematic liquid crystal 4′-(*n*-pentyl)-4-cyanobiphenyl (5CB) doped with a small amount of the laser dye rhodamine 6G (R6G) which worked as the charge generator. A schematic representation of the experimental geometry is illustrated in figure 21. The Ar^+ coherent laser beam is split into two beams that overlap at a small angle θ in the sample which, in turn, is tilted at an angle β to the bisector of θ. This creates an optical interference pattern of the form $I = I_0[1 + \cos(qx)]$ which photogenerates charge carriers and allows charge migration along the grating wavevector $\boldsymbol{q}$ and trapping in the dark region of the interference pattern. The result in a sinusoidally modulated space-charge field given by equation (113)

$$E_{sc} = \frac{-mk_BTq}{2e}\left(\frac{D^+ - D^-}{D^+ + D^-}\right)\frac{\sigma - \sigma_d}{\sigma}\sin(qx) = E_{sc}^{(0)}\sin(qx) \tag{113}$$

where m is the modulation index of the interference pattern, σ is the illuminated state conductivity (i.e. the photoconductivity), σ_d is the dark state conductivity, k_B is the Boltzmann constant, e is the proton charge and D^+ and D^- are the diffusion constants for the cations and anions, respectively [105, 106]. Notice that E_{sc} (which varies as $\sin qx$) is $\pi/2$ phase shifted from the optical grating function ($\sim \cos qx$). Two factors determine the magnitude of the space-charge field in equation (113): the difference between σ and σ_d, and the difference in the diffusion coefficients of the cations and anions. The externally applied field $\boldsymbol{E}_0$, which is greater in magnitude than the internal space-charge field, is required to keep the modulation of the internal electric field greater than zero. Coupling between the space-charge field and the uniform dc bias field $\boldsymbol{E}_0$ causes reorientation of the LC director and correspondent modulation of the refractive index. The application of an electric field of only 100–200 V cm^{-1} is sufficient to induce directional charge transport and to induce a grating spacing for the orientational grating equal to the interference pattern [104–106]. The diffraction efficiency of this Raman-Nath orientational grating can be written as [105, 106]

$$\eta = \left[\frac{Lmk_BT}{\lambda n_e Kqe}\left(\frac{E_a\varepsilon_s\varepsilon_\infty \sin\beta\cos\beta}{1 + \varepsilon_s E_a^2/(2\pi Kq^2)}\right)\frac{D^+ - D^-}{D^+ + D^-}\frac{\sigma - \sigma_d}{\sigma}\right]^2 \tag{114}$$

where L is the sample thickness, n_e is the index of refraction along the extraordinary axis, K is the Frank elastic constant in the single constant approximation [29], λ is the laser wavelength, ε_s is the static dielectric constant and ε_∞ is the high-frequency dielectric constant. Rudenko and Sukhov showed that the conductivity term in equation (114) saturates at high light intensities and this allowed them to determine experimentally the ratio $(D^+ - D^-)/(D^+ + D^-)$. The value of 0.02 found for this ratio indicated a very small difference in the diffusion coefficients of the positive and negative mobile ions. This fact, combined with the low solubility of the laser dye and the inefficient charge generation and charge transport, strongly limited the performances

of the material. Significant improvements of the PR performances were obtained by doping the nematic LCs with both electron donors and acceptors having appropriate redox characteristics that produce more efficient intermolecular charge separation and bulk charge migration [102].

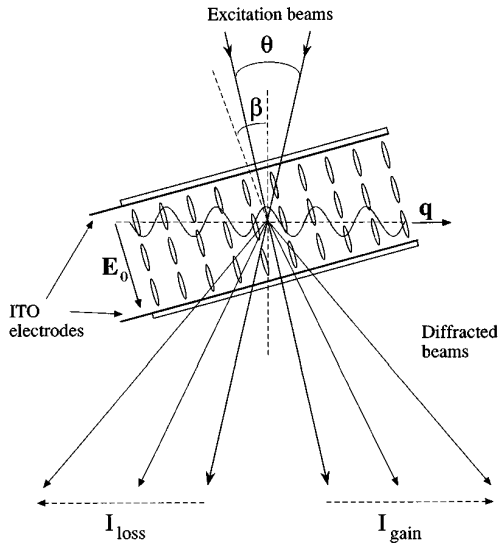

Figure 21. Schematic representation of the experimental geometry used to observe the photorefractive effect in LCs. A coherent laser beam is split into two beams that overlap at a small angle θ in the sample. The sample is tilted at an angle β to the bisector of the two beams. $\boldsymbol{E}_0$ is the dc external electric field. This configuration makes possible charge migration along the grating wavevector $\boldsymbol{q}$, which results in a sinusoidal space-charge field. The action of the space-charge field on the orientational configuration of the birefringent molecules produces the phase grating. The direction of $\boldsymbol{q}$ defines the x axis.

Recently, a PR effect that was derived entirely from orientational ordering within a space charge field was reported by Khoo and coworkers in pure aligned nematic liquid crystals (NLCs) [107]. The geometry of their experiment is similar to that used by Rudenko and Sukhov [104] reported in figure 21. The molecular reorientation effects were observed in undoped or lightly doped [108] films of several nematic LCs, including single constituent nematics and nematic mixtures. The induced nonlocal refractive-index change responsible for these effects was attributed to LC director axis reorientation induced by a laser-induced dc space-charge field arising from both conductivity and dielectric anisotropies, in the presence of an applied dc electric field.

In nematic LCs several mechanisms contribute to the creation of a space-charge field. Space-charge fields can be induced by an applied dc field as a result of the conductivity and dielectric anisotropies; this is known as the Carr–Helfrich effect [109]. In addition, a space charge field can be set up via the photocharge production (which is responsible for the observed photoinduced conductivity change), similar to the process occurring in photorefractive crystals. These space-charge fields create torques that reorient the LC director to produce reorientation grating for the LC director. A theoretical discussion of the fundamental mechanisms regulating the dc field-assisted optically induced space-charge fields and the optical molecular reorientation in nematic LC films has been reported by Khoo in reference [110]. Three processes contribute to the director axis reorientation and

the consequent refractive index change. The first one (involving photo-charge production, ions drift/diffusion, charge separation and space-charge field formation) is analogous to those occurring in photorefractive crystals and leads to the photorefractive-like space charge field $\boldsymbol{E}_{sc}$ ($\boldsymbol{E}_{sc} = E_{sc}\boldsymbol{u}_x$) expressed by equation (113). The second process involves charge generation, ionic conduction accompanied by director axis reorientation, space charge field formation through dielectric and conductivity anisotropy and further director axis reorientation. Finally, the steps involved in the third process are charge generation, material flows, formation of a velocity gradient and shear stress and director axis reorientation. These latter processes are unique to NLCs and are consequence of the Carr–Helfrich effect occurring in these materials. Figure 22 shows a schematic depiction of various parameters involved in the nonlinear photorefractive effect in LCs. Assuming an incident optical intensity distribution of the form $I = I_0(1 + \cos \boldsymbol{q} \cdot \boldsymbol{r}) = I_0(1 + \cos qx)$ and an applied dc field E_0 directed along the y axis, the behaviour of the corresponding director axis reorientation profile $\theta(x)$, the currents and the liquid flow velocity are schematically represented in the figure. Following the theory of Helfrich [109] for the geometry of figure 22, the space-charge field arising from dc conductivity anisotropy $\Delta\sigma$ ($\Delta\sigma = \sigma_\parallel - \sigma_\perp$) can be shown to be [110] $\boldsymbol{E}_{\Delta\sigma} = E_{\Delta\sigma}\boldsymbol{u}_x$, with

$$E_{\Delta\sigma} = -\left(\frac{\Delta\sigma \sin\theta\cos\theta}{\sigma_\parallel \sin^2\theta + \sigma_\perp \cos^2\theta}\right) E_0 \tag{115}$$

whereas the space-charge field due to the dielectric anisotropy $\Delta\varepsilon$ ($\Delta\varepsilon = \varepsilon_\parallel - \varepsilon_\perp$) is $\boldsymbol{E}_{\Delta\varepsilon} = E_{\Delta\varepsilon}\boldsymbol{u}_x$:

$$E_{\Delta\varepsilon} = -\left(\frac{\Delta\varepsilon \sin\theta\cos\theta}{\varepsilon_\parallel \sin^2\theta + \varepsilon_\perp \cos^2\theta}\right) E_0. \tag{116}$$

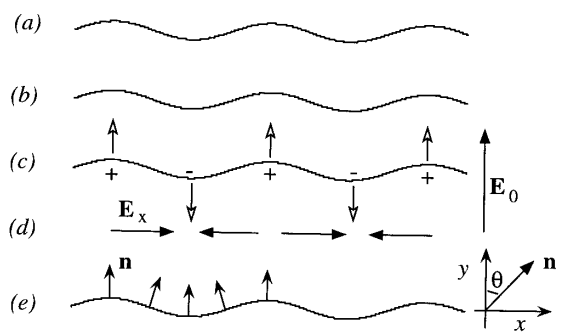

Figure 22. Schematic representation of the quantities involved in the nonlinear photorefractive effect: (a) input optical intensity; (b) photoinduced conductivity modulation; (c) flow velocity and space charge; (d) dc space-charge field; (e) director axis reorientation profile. $\boldsymbol{n}$ is normal to the curve and θ is the reorientation angle. (After Khoo [108].)

We observe that these space-charge fields are both increasing functions of the induced reorientation angle θ, for small θ. A small initial reorientation angle and space-charge field will thus reinforce each other; once the reorientation is established, we can see from equations (115) and (116) that the space-charge field can be maintained by simply applying the dc field, without participation from the incident optical field at all. Such effect was actually observed by Khoo in his reported study [108] of the holographic grating formation dynamics.

These fields and space charges, in conjunction with the applied dc field, create director axis reorientation through several mechanisms. The interaction of the space charges ($\sim \cos qx$)

with the applied field causes nematic flows in opposite directions, with positive and negative charges flowing with velocities v_z and $-v_z$, respectively. The flow gradient $\mathrm{d}v_z/\mathrm{d}x$ gives rise to a flow-shear stress which, in turn, exerts a torque on the molecules of the LC. This *shear-induced* torque Γ_S is given by [111, 112]

$$\Gamma_S = -\frac{\mathrm{d}v_z(x)}{\mathrm{d}x}[\alpha_3 \cos^2\theta - \alpha_2 \sin^2\theta] \tag{117}$$

where α_2 and α_3 are the Leslie coefficients.

The shear torque Γ_S tends to change the direction of the preferred axis and thus reacts on the orientation pattern. Its effect is reorientation of the director axis that follows the modulation of the flow gradient ($\sim \sin qx$).

The space charges also influence the director axis reorientation through the electric fields which they produce. These fields, in conjunction with the applied dc field, create a *dielectric* torque $\mathbf{\Gamma}_{\Delta\varepsilon}$ of the form [112]

$$\mathbf{\Gamma}_{\Delta\varepsilon} = \frac{\Delta\varepsilon}{4\pi}(\boldsymbol{n}\cdot\boldsymbol{E}_{dc})(\boldsymbol{n}\times\boldsymbol{E}_{dc}) = \frac{\Delta\varepsilon}{4\pi}[\sin\theta\cos\theta(E_x^2 - E_0^2) + \cos 2\theta E_x E_0] \tag{118}$$

where E_x is the x component of the total dc electric field $\boldsymbol{E}_{dc}$

$$\boldsymbol{E}_{dc} = (E_{sc} + E_{\Delta\sigma} + E_{\Delta\varepsilon})\boldsymbol{u}_x + E_0\boldsymbol{u}_y. \tag{119}$$

This torque also gives rise to a spatially phase-shifted director axis reorientation similar to the flow-induced effect. The total conduction-induced torque is, therefore, partly shear induced and partly dielectric.

The dynamics of the director axis reorientation process is governed by interplay among the various torques produced by the fields and the elasticity of the liquid crystal and is described by the equation

$$\Gamma_{\Delta\varepsilon} + \Gamma_S + \Gamma_K + \Gamma_{OPT} + \gamma\frac{\mathrm{d}\theta}{\mathrm{d}t} = 0 \tag{120}$$

where Γ_{OPT} is the classical optical torque, $\gamma\,\mathrm{d}\theta/\mathrm{d}t$ is a viscous damping term which accounts for the dissipation of mechanical energy caused by friction during the reorientation process (γ is an appropriate interaction-geometry dependent viscosity coefficient) and Γ_K is the elastic restoring torque. In this experimental geometry this latter can be written as [28, 29]

$$\Gamma_K = (K_1\sin^2\theta + K_3\cos^2\theta)\left(\frac{\partial^2\theta}{\partial x^2} + \frac{\partial^2\theta}{\partial z^2}\right) + [(K_1 - K_3)\sin\theta\cos\theta]\left[\left(\frac{\partial\theta}{\partial x}\right)^2 + \left(\frac{\mathrm{d}\theta}{\partial z}\right)^2\right] \tag{121}$$

where K_1 and K_3 are the elastic constants for splay and bend, respectively. The steady state ($\mathrm{d}\theta/\mathrm{d}t = 0$) solution of the torque balance equation (121) can be easily found if we limit our analysis to small reorientation angles in the one elastic constant approximation ($K_1 = K_3 = K$). Within this assumptions and rewriting the flow-orientation torque as (by applying the Poisson's equation, the equation of continuity and the viscous force equation) [112]

$$\Gamma_\sigma = \frac{\alpha_3}{\eta_2}\frac{\Delta\sigma}{\sigma_\parallel}\frac{\varepsilon_\perp}{4\pi}E_z^2\theta \tag{122}$$

equation (120) reduces to [110]

$$K\left(\frac{\partial^2\theta}{\partial x^2} + \frac{\partial^2\theta}{\partial z^2}\right) + \frac{\Delta\varepsilon}{4\pi}E_z E_{sc}^{(0)}\cos\beta\sin(qx) + \frac{\Delta\varepsilon}{4\pi}E_z^2\left[1 + \frac{\alpha_3}{\eta_2}\frac{\Delta\sigma}{\sigma_\parallel}\frac{\varepsilon_\perp}{\Delta\varepsilon} + \left(\frac{\Delta\varepsilon}{\varepsilon_\perp} + \frac{\Delta\sigma}{\sigma_\perp}\right)\cos\beta\right]\theta = 0 \tag{123}$$

where η_2 is the viscosity coefficient of the nematic fluid for $\boldsymbol{n}$ parallel to the flow velocity ($\eta_2 = [\alpha_3 + \alpha_4 + \alpha_6]/2$, α_i being the Leslie coefficients). The boundary conditions over the glass plates limiting the homeotropically aligned LC cell impose $\theta(0) = \theta(d) = 0$. Then, writing the reorientation angle θ as

$$\theta = \theta_0 \sin\left(\frac{\pi y}{d}\right) \sin(qx) \tag{124}$$

equation (123) can be solved to give

$$\theta_0 = \frac{\Delta\varepsilon E_z E_{sc}^{(0)} \cos\beta}{K(\pi^2/d^2 + q^2) + (\Delta\varepsilon/4\pi)E_z^2[1 + (\alpha_3/\eta_2)(\Delta\sigma/\sigma_\parallel)\varepsilon_\perp/\Delta\varepsilon + (\Delta\varepsilon/\varepsilon_\perp + \Delta\sigma/\sigma_\perp)\cos\beta]}. \tag{125}$$

The quadratic dependence of the field-induced torque (118) reflects into the appearance of the field product in equation (125). Finally, under the small θ_0 approximation, one finds for the refractive index change

$$\Delta n \approx (n_\parallel - n_\perp)\frac{n_\parallel}{n_\perp}(\sin 2\beta)\theta_0 \tag{126}$$

which reveals the quadratic nature of this electrooptic effect. Since the diffraction efficiency η is proportional to the square of Δn, the β dependence of η according to equations (125) and (126) is of the form $\sin^2\beta\cos^4\beta$. This results in good agreement with the experimental observations as reported by Khoo in [107].

It is interesting to make a qualitative comparison between the reorientational effects due to optically induced dc fields with those due to purely optical fields. In the experiments of Khoo with the 5CB nematic liquid crystal, for instance, optical powers of the order of 200 mW were required to obtain a diffraction efficiency of 1% in the case of purely optical fields, whereas an optical power of only 10 mW was needed in the presence of optically induced dc fields. The key factor for the larger orientational efficiency of the dc field is the large magnitude of the dielectric anisotropy $\Delta\varepsilon$ ($\sim$20 for 5CB) compared to the optical anisotropy $\Delta\varepsilon_{op}$ ($\sim$0.6 for 5CB).

The time evolution of the above described mechanisms underlying the photorefractive effect have also been examined by Khoo and coworkers in connection with the investigation of the holographic formation in dye- and fullerene C_{60}-doped nematic LCs [108, 110]. In particular, under low optical writing beam power (few milliwatts) and low applied voltage ($\leqslant$1.5 V), the time evolution and nature of the induced grating (as monitored by the diffraction of the probe He–Ne laser) exhibited three distinct stages depending on the illumination time. For short illumination time (few seconds) the induced grating was transient, with rise and decay time constants of the order of 1 second, which is typical of the orientational decay time in LC films with thickness of a few tenths of microns [108]. If the writing beams were kept on after the initial quasi-stationary value was reached, it was observed that the probe diffraction slowly but steadily increased in magnitude before settling down to a final steady-state value after 15–20 minutes. If the writing beams were turned off before the final steady state was reached while maintaining the dc field, the probe diffraction was observed to drop to a lower value. The diffraction persisted as long as the dc field was kept on and decayed slowly (in a few minutes) to a lower finite value. If the dc field was abruptly turned off during this decay period, the grating relaxed in about 1 second, which is the characteristic time of the director axis relaxation time mentioned above. This intermediate stage was interpreted as corresponding to the case when the reorientation angle acquires a sufficiently large magnitude so that the dc-applied-field-dependent space-charge fields $E_{\Delta\sigma}$ (equation (115)) and $E_{\Delta\varepsilon}$ (equation (116)) become substantial. Different from the photorefractive space-charge field E_{sc} (equation (113)), these

space-charge fields depend only on the reorientational angle and the dc applied field but *not* on the incident optical field; this explains why part of the grating can be sustained by the dc field when the writing beams are turned off. The final stage in the grating formation is reached for an illumination time greater than 15 minutes. Then, if all external applied fields are turned off, a persistent grating remains. In the Rhodamine 6G (R6G) dye-doped LC (5CB) sample the grating was found to decay in about two hours whereas in the fullerene C_{60}-doped LC (5CB) sample the grating was revealed to be permanent.

Based upon the same effect of director axis reorientation due to optically induced space-charge fields, an extraordinarily large optically induced refractive index change mechanism has recently been observed in aligned dye-doped nematic LCs [113]. Grating diffraction could be generated in these materials with an optical intensity as low as 40 μW cm^{-2}, and a refractive-index change coefficient of over 6 cm^2 W^{-1} was obtained. This sensitivity rivals those obtainable from a conventional LC light valve or spatial light modulator. Besides the development of new LC light valves and spatial light modulators, the effect is extremely promising for applications in other adaptive optics and coherent wave-mixing devices.

5. Conclusions

We have reviewed basic physical mechanisms underlying the light-induced molecular reorientation in nematic LCs, namely direct optical torque, photoisomerization and photorefractivity.

We have seen that in transparent materials the observed effects of molecular reorientation can be fully interpreted within the framework of classical electrodynamics and standard continuum theory of LCs. A detailed description of this approach has been reported. The electromagnetic field exerts a torque on the LC molecules due to their anisotropic molecular polarizability. This torque is balanced by the elastic and viscous torque associated with the spatial nonuniformity and rotation, respectively, of the nematic director. What makes LCs peculiar with respect to other materials constituted of anisotropic molecules is their ability to preserve the anisotropy on a macroscopic scale. Related to the macroscopic anisotropy and the collective behaviour of these materials, reorientational effects much stronger than in conventional anisotropic materials can be observed, that lead to extraordinarily large NLO response. We have reviewed the main properties of the light-induced phenomena which strongly affect the macroscopic order of LCs.

In the presence of light absorption, however, new effects take place that cannot be interpreted with the help of the macroscopic phenomenological theory. In fact, LCs play a peculiar role in the general outline of photoactive media because their fluidity maintains the possibility of molecular motion in response to photon absorption, while their orientational ordering offers the possibility of cooperative behaviour that can amplify relatively weak photochemical effects. Small amounts ($\sim$1%) of absorbing dye added to nematic LCs lead to an increase of the optical torque up to two orders of magnitude. The strength and sign of this additional absorption-induced torque is strictly connected to the nature of the dye, for some dyes having the same sign as the dielectric optical torque while for others being different. In order to explain these effects, molecular models have been elaborated based upon the assumption that in the presence of absorption the orientational distributions of the ground-state and excited-state dye molecules are not axially symmetric around the director. This asymmetry causes the mean field of the dye to exert an effective torque on the director due to both the change of the dye–host interaction energy upon excitation and the difference between the rotational mobility of the ground-state and the excited-state molecules. These models successfully describe the experimental evidences for many guest–host systems and

account for the strong optical torque enhancement. However, they do not describe the complex phenomenology that is observed when the dye molecules consist of azobenzene derivatives. In this case, it is the photoisomerization process that drives the evolution of the dye–LC system consequent to the interaction with the light. A detailed report of the experimental evidence connected to the process of optical reorientation in the presence of photoisomerization and of the physical mechanisms that allow to interpret them has been reported in this paper.

Finally, the relatively new field of photorefractivity in LCs has been considered. A crucial role in the reorientation process in photorefractive materials is played by the space-charge field that originates from the interaction of the material with a spatially modulated intensity distribution of light. The different mechanisms contributing to the creation of a space-charge field, such as conductivity anisotropy, dielectric anisotropy and photocharge production, have been reviewed in detail. The space-charge fields create torques that reorient the LC director to produce reorientation grating for the LC director. A theoretical discussion of the fundamental mechanisms regulating the dc-field-assisted optically induced space-charge fields and the optical molecular reorientation in nematic LC films have also been reported.

We believe that at the present state of knowledge direct optical torque due to light field, molecular photo-transformation and photo-induced charge generation are the basic phenomena occurring in the interaction of light with LCs. Connected to these, several fundamental aspects have yet to be clarified whose investigation will provide new ideas for innovative applications in the field of optical processing and optical storage.

Acknowledgments

It is a pleasure to thank Dr D Lucchetta for his valuable help in the preparation of some of the figures.

References

[1] Zel'dovich B Ya, Pilipetskii N F, Sukhov A V and Tabiryan N V 1980 *JETP Lett.* **31** 264
[2] Khoo I C and Zhuang S L 1980 *Appl. Phys. Lett.* **37** 3
[3] Zolot'ko A S, Kitaeva V F, Kroo N, Sobolev N I and Csillag L 1980 *JETP Lett.* **32** 158
[4] Durbin S D, Arakelian S M and Shen Y R 1981 *Phys. Rev. Lett.* **47** 1411
[5] Pilipetskii N F, Sukhov A V, Tabiryan N V and Zel'dovich B Ya 1981 *Opt. Commun.* **37** 280
[6] Khoo I C, Zhuang S L and Shepard S 1981 *Appl. Phys. Lett.* **39** 937
[7] Khoo I C 1981 *Appl. Phys. Lett.* **38** 123
[8] Khoo I C 1981 *Phys. Rev.* A **23** 2077
[9] Zolot'ko A S, Kitaeva V F, Kroo N, Sobolev N I and Csillag L 1981 *JETP Lett.* **34** 250
[10] Zolot'ko A S, Kitaeva V F, Sobolev N I and Sukhorukov A P 1981 *Sov. Phys.–JETP* **81** 933
[11] Khoo I C and Zhuang S L 1982 *IEEE J. Quantum Electron.* **18** 246
[12] Csillag L, Jánossy I, Kitaeva V F, Kroo N and Sobolev N N 1982 *Mol. Cryst. Liq. Cryst.* **84** 125
[13] Khoo I C 1982 *Phys. Rev.* A **25** 1636
[14] Khoo I C 1982 *Phys. Rev.* A **25** 1040
[15] Durbin S D, Arakelian S M and Shen Y R 1982 *Opt. Lett.* **7** 145
[16] Santamato E and Shen Y R 1984 *Opt. Lett.* **9** 564
[17] Simoni F and Bartolino R 1985 *Opt. Commun.* **53** 210
[18] Umeton C, Sgro' A and Simoni F 1987 *J. Opt. Soc. Am.* B **4** 1938
[19] Khoo I C, Hou J Y, Liu T H, Yan P Y, Michael R R and Finn G M 1987 *J. Opt. Soc. Am.* B **4** 886
[20] Santamato E, Abbate G, Calselice R, Maddalena P and Sasso A 1988 *Phys. Rev.* A **37** 1375
[21] Bloisi F, Vicari L, Simoni F, Cipparrone G and Umeton C 1988 *J. Opt. Soc. Am.* B **5** 2462
[22] Cipparrone G, Versace C, Bloisi F, Vicari L and Simoni F 1988 *Nuovo Cimento* D **10** 1235
[23] Khoo I C and Liu T H 1989 *Phys. Rev.* A **39** 4036
[24] Drevensek I and Copic M 1991 *Mol. Cryst. Liq. Cryst.* **207** 241
[25] Khoo I C 1991 *Mol. Cryst. Liq. Cryst.* **207** 317

[26] Chen S H and Luo C L 1991 *Mol. Cryst. Liq. Cryst.* **207** 131
[27] Khoo I C, Wang W, Simoni F, Cipparrone G and Duca D 1991 *J. Opt. Soc. Am.* B **8** 1433
[28] Simoni F 1997 *Nonlinear Optical Properties of Liquid Crystals and PDLC* (Singapore: World Scientific)
[29] De Gennes P G 1974 *The Physics of Liquid Crystals* (Oxford: Oxford University Press)
De Gennes P G and Prost J 1993 *The Physics of Liquid Crystals* (Oxford: Oxford University Press)
[30] Zel'dovich B Ya and Tabiryan N V 1982 *Sov. Phys.–JETP* **55** 656
[31] Tabiryan N V, Sukhov A V and Zel'dovich B Ya 1986 *Mol. Cryst. Liq. Cryst.* **136** 1
[32] Santamato E, Abbate G and Maddalena P 1988 *Phys. Rev.* A **38** 4323
[33] Santamato E, Abbate G, Maddalena P and Shen Y R 1988 *Phys. Rev.* A **36** 2389
[34] Abbate G, Maddalena P, Marrucci L, Saetta L and Santamato E 1991 *J. Physique* II **1** 543
[35] Santamato E, Daino B, Romagnoli M, Settembre M and Shen Y R 1986 *Phys. Rev. Lett.* **57** 2423
[36] Santamato E, Abbate G, Maddalena P, Marrucci L and Shen Y R 1990 *Phys. Rev. Lett.* **64** 1377
[37] Santamato E, Abbate G, Maddalena P, Marrucci L and Shen Y R 1990 *Mol. Cryst. Liq. Cryst.* **179** 189
[38] Santamato E, Abbate G, Maddalena P, Marrucci L and Shen Y R 1991 *Mol. Cryst. Liq. Cryst.* **198** 225
[39] Abbate G, Maddalena P, Marrucci L, Saetta L and Santamato E 1991 *Mol. Cryst. Liq. Cryst.* **207** 161
[40] Abbate G, Santamato E and Maddalena P 1988 *Nuovo Cimento* D **10** 313
[41] Abbate G, Maddalena P, Marrucci L and Santamato E 1991 *J. Appl. Phys.* **69** 1269
[42] Cipparrone G, Carbone V, Versace C, Umeton C, Bartolino R and Simoni F 1993 *Phys. Rev.* E **47** 3741
[43] Jánossy I, Lloyd A D and Wherrett B S 1990 *Mol. Cryst. Liq. Cryst.* **179** 1
[44] Jánossy I and Lloyd A D 1991 *Mol. Cryst. Liq. Cryst.* **203** 77
[45] Jánossy I, Csillag L and Lloyd A D 1991 *Phys. Rev.* A **44** 8410
[46] Jánossy I and Kosa T 1992 *Opt. Lett.* **17** 1183
[47] Jánossy I 1994 *Phys. Rev.* E **49** 2957
[48] Kosa T and Jánossy I 1995 *Opt. Lett.* **20** 1230
[49] Marrucci L and Paparo D 1997 *Phys. Rev.* E **56** 1765
[50] Rau H 1990 *Photochemistry and Photophysics* vol 2 ed F J Rabeck (Boca Raton, FL: Chemical Rubber Company) ch 4 pp 119–41
[51] Blinov L M 1996 *J. Nonlin. Opt. Phys. Mater.* **5** 165
[52] Sekkat Z, Büchel M, Orendi H, Menzel H and Knoll W 1994 *Chem. Phys. Lett.* **220** 497
[53] Anderle K and Wendorff J H 1994 *Mol. Cryst. Liq. Cryst.* **243** 51
[54] Sekkat Z, Wood J, Aust E F, Knoll W, Volksen W and Miller R D 1996 *J. Opt. Soc. Am.* B **13** 1713
[55] Ichimura K, Suzuzki Y, Seki T, Hosoki A and Aoki K 1988 *Langmuir* **4** 1214
[56] Gibbons W M, Kòsa T, Palffy-Muhoray P, Shannon P J and Sun T S 1995 *Nature* **377** 43
[57] Dumont M 1996 *Nonlin. Opt.* **15** 59
[58] Todorov T, Nikolova L and Tomova N 1984 *Appl. Opt.* **23** 4309 and references therein
[59] Läsker L, Fischer T, Stumpe J, Kostromin S, Ivanov S, Shibaev V and Ruhmann R 1994 *Mol. Cryst. Liq. Cryst.* **246** 1; 347
[60] Palto S P, Shtykov N M, Khavrichev V A and Yudin S G 1992 *Mol. Mater.* **1** 3
[61] Khoo I C and Wu S T 1993 *Optics and Nonlinear Optics of Liquid Crystals* (Singapore: World Scientific) ch 1.9.3
[62] Anderle K, Birenheide R, Werner M J A and Wendorf J H 1991 *Liq. Cryst.* **9** 691
[63] Ivanov S, Yakolev I, Kostromin S, Shibaev V, Läsker L, Stumpe J and Kreysig D 1991 *Macromol. Chem. Rapid Commun.* **12** 709
[64] Anderle K and Wendorff J H 1994 *Mol. Cryst. Liq. Cryst.* **243** 51 and references therein
[65] Birenheide R and Wendorff J H 1990 *Proc. SPIE* **1213** 89
[66] Odulov S G, Reznikov Yu A, Soskin M S and Khizhnyak A I 1983 *Sov. Phys.–JETP* **58** 1154
[67] Chen A G and Brady D J 1992 *Opt. Lett.* **17** 441
[68] Ikeda T and Tsutsumi O 1995 *Science* **268** 1873
[69] Folks R W, Reznikov Yu, Chen L, Khiznyak A I and Lavrentovich O D 1995 *Mol. Cryst. Liq. Cryst.* **261** 259
[70] Gibbons W M, Shannon P J, Sun S T and Sweltin B J 1991 *Nature* **351** 49
[71] Ichimura K, Hayashi Y, Ikeda T, Akiyama H and Ishizuki N 1993 *Appl. Phys. Lett.* **63** 449
[72] Ichimura K and Akiyama H 1993 *Makromol. Chem. Rapid Commun.* **14** 813
[73] Iimura Y, Kusano J, Kobayashi S, Aoyagi Y and Sugano T 1993 *Japan. J. Appl. Phys.* 2 **32** L93
[74] Chen A G and Brady D J 1993 *J. Appl. Phys. Lett.* **62** 2920
[75] Sun S T, Gibbons W M and Shannon P J 1992 *Liq. Cryst.* **12** 869
[76] Eich M, Wendorff J H, Reck B and Ringsdorf H 1987 *Makromol. Chem. Rapid Commun.* **8** 59
[77] Anderle K, Birenheide R, Werner M J A and Wendorff J H 1991 *Liq. Cryst.* **9** 691
[78] Marusii T, Reznikov Y, Voloshcheenko D and Reshetnyak V 1994 *Mol. Cryst. Liq. Cryst.* **251** 209

[79] Voloshchenko D, Khyzhnyak A, Reznikov Y and Reshetnyak V 1995 *Japan. J. Appl. Phys.* **34** 566
[80] Blinov L M, Barnik M I, Mazzulla A and Umeton C 1995 *Mol. Mater.* **5** 237
[81] Marusii T Ya, Reznikov Yu A and Slussarenko S S 1996 *Mol. Mater.* **6** 163
[82] Simoni F, Francescangeli O, Reznikov Y and Slussarenko S 1997 *Opt. Lett.* **22** 549
[83] Slussarenko S, Francescangeli O, Simoni F and Reznikov Y 1997 *Appl. Phys. Lett.* **71** 3613
[84] Simoni F, Francescangeli O, Pepe I, Reznikov Y and Slussarenko S 1998 *Proc. SPIE* **3318** 258
[85] Francescangeli O, Simoni F, Slussarenko S, Andrienko D, Reshetnyak V and Reznikov Y 1999 *Phys. Rev. Lett.* **82** 1855
[86] Khoo I C, Shin M-Y, Wood M V, Guenther B D, Chen P H, Simoni F, Slussarenko S S, Francescangeli O and Lucchetti L 1999 *Proc. IEEEE (November 1999)* vol 57 (11)
[87] Petri A, Kummer S, Anneser H, Feiner F and Bräuchle Ch 1993 *Ber. Bunsenges. Phys. Chem.* **97** 1281
[88] Dumont M, Froc G and Hosotte S 1995 *Nonlin. Opt.* **9** 327
[89] Jánossy I and Szabados L 1998 *Phys. Rev.* E **58** 4598
[90] Barnik M I, Zolot'ko A S, Rumyantsevn V G and Terskov D B 1995 *Kristallografiya* **40** 746
[91] Jánossy I and Szabados L 1998 *J. Nonlin. Opt. Phys. Mater.* **7** 539
[92] Saad B, Galstyan T V, Denariez-Roberge M M and Dumont M 1998 *Opt. Comm.* **151** 235
[93] Li H, Liang Y and Khoo I C 1994 *Mol. Cryst. Liq. Cryst.* **251** 85
[94] Ashkin A, Boyd G, Dziedzic J M, Smith R G, Ballman A A, Levinstein J J and Nassau K 1966 *Appl. Phys. Lett.* **9** 72
[95] Gunter P and Huignard J P 1988 and 1989 *Photorefractive Materials and Their Applications I* vols 1 and 2 (Berlin: Springer)
[96] Born M and Wolf E 1975 *Principles of Optics* (London: Pergamon)
[97] Ducharme S, Scott J C, Twieg J and Moemer W E 1991 *Phys. Rev. Lett.* **66** 1846
[98] Silence S M, Scott J C, Stankus J J, Moerner W E, Moylan C R, Bjorklund G C and Twieg R J 1995 *J. Phys. Chem.* **99** 4096
[99] Moerner W E, Silence S M, Hache F and Bjorklund G C 1994 *J. Opt. Soc. Am.* B **11** 320
[100] Meerholz K, Volodin B L, Sandalphon, Kippelen B and Peyghambarian N 1994 *Nature* **371** 497
[101] Moerner W E and Silence S M 1994 *Chem. Rev.* **94** 127
[102] Wiederrecht G P, Yoon B A and Wasielewski M R 1995 *Science* **270** 1794
[103] Wiederrecht G P, Yoon B A and Wasielewski M R 1996 *Adv. Mater.* **8** 535
[104] Rudenko E V and Sukhov A V 1994 *JETP Lett.* **59** 142
[105] Rudenko E V and Sukhov A V 1994 *Sov. Phys.–JETP* **78** 875
[106] Rudenko E V and Sukhov A V 1996 *Mol. Cryst. Liq. Cryst.* **282** 125
[107] Khoo I C, Li H and Liamg Y 1994 *Opt. Lett.* **19** 1723
[108] Khoo I C 1995 *Opt. Lett.* **20** 2137
[109] Helfrich W 1969 *J. Chem. Phys.* **51** 4092
[110] Khoo I C 1996 *Mol. Cryst. Liq. Cryst.* **282** 53
[111] Hsiung H, Shi L P and Shen Y R 1984 *Phys. Rev.* A **30** 1453
[112] Khoo I C 1994 *Liquid Crystals: Physical Properties and Nonlinear Optical Phenomena* (New York: Wiley–Interscience)
[113] Khoo I C, Slussarenko S, Guenther B D, Shih Min-Yi, Chen P H and Wood W V 1998 *Opt. Lett.* **23** 253